

Visual motion and form integration in the behaving ferret

<https://doi.org/10.1523/ENEURO.0228-19.2019>

Cite as: eNeuro 2019; 10.1523/ENEURO.0228-19.2019

Received: 14 June 2019

Revised: 10 July 2019

Accepted: 14 July 2019

This Early Release article has been peer-reviewed and accepted, but has not been through the composition and copyediting processes. The final version may differ slightly in style or formatting and will contain links to any extended data.

Alerts: Sign up at www.eneuro.org/alerts to receive customized email alerts when the fully formatted version of this article is published.

Copyright © 2019 Dunn-Weiss et al.

This is an open-access article distributed under the terms of the Creative Commons Attribution 4.0 International license, which permits unrestricted use, distribution and reproduction in any medium provided that the original work is properly attributed.

Title: Visual motion and form integration in the behaving ferret

Abbreviated title: Motion and form integration in the ferret

Authors: Erika Dunn-Weiss^{1,2}, Samuel U. Nummela^{1,2}, Augusto A. Lempel^{1,2}, Jody Law², Johanna Ledley², Peter Salvino², Kristina J. Nielsen^{1,2}

Affiliations: ¹ Solomon H. Snyder Department of Neuroscience, Johns Hopkins University School of Medicine, Baltimore, MD 21205, USA

² Zanvyl Krieger Mind/Brain Institute, Johns Hopkins University, Baltimore, MD 21218, USA

Author contributions: EDW, SUU and KJN designed research; EDW and SUU performed research and analyzed data; AAL, JLaw, JLedley and PS performed research; EDW and KJN wrote the paper.

Corresponding author: Kristina J. Nielsen
Kristina.nielsen@jhmi.edu

Number of figures: 7

Number of tables: 3

Number of multimedia: 0

Number of words for abstract: 225

Number of words for significance statement: 118

Number of words for introduction: 643

Number of words for discussion: 1297

Acknowledgments: This work was supported by a grant from the Science of Learning Institute at JHU, and grant from the National Eye Institute (EY027853). We thank S. Niziolek, O. Garalde, J. Killebrew, W. Nash and W. Quinlan for technical support. We are grateful to the Cohen lab at JHU for helpful discussions of the head-fixed setup design, and to all Nielsen and Connor lab members for general discussions and experimental support. We thank A. A. Disney for her comments on the manuscript. SUN current address: Truckee Meadows Community College, Department of Biology, Reno, NV 89512, USA

JLaw current address: Washington University School of Medicine, St. Louis, MO 63110, USA

JLedley current address: Brigham and Women's Hospital, Boston MA, 02115, USA

Conflict of interest: The authors report no conflict of interest.

Funding sources: National Eye Institute grant EY027853, Science of Learning Institute at JHU

41 Abstract

42 Ferrets have become a standard animal model for the development of early visual stages. Less is known
43 about higher-level vision in ferrets, both during development and in adulthood. Here, as a step towards
44 establishing higher-level vision research in ferrets, we used behavioral experiments to test the motion
45 and form integration capacity of adult ferrets. Motion integration was assessed by training ferrets to
46 discriminate random dot kinematograms (RDK) based on their direction. Task difficulty was varied
47 systematically by changing RDK coherence levels, which allowed the measurement of motion integration
48 thresholds. Form integration was measured analogously by training ferrets to discriminate linear Glass
49 patterns of varying coherence levels based on their orientation. In all experiments, ferrets proved to be
50 good psychophysical subjects that performed tasks reliably. Crucially, the behavioral data showed clear
51 evidence of perceptual motion and form integration. In the monkey, motion and form integration are
52 usually associated with processes occurring in higher-level visual areas. In a second set of experiments,
53 we therefore tested whether PSS, a higher-level motion area in the ferret, could similarly support
54 motion integration behavior in this species. To this end, we measured responses of PSS neurons to RDK
55 of different coherence levels. Indeed, neurometric functions for PSS were in good agreement with the
56 behaviorally derived psychometric functions. In conclusion, our experiments demonstrate that ferrets
57 are well suited for higher-level vision research.

58

59 Significance statement

60 The ferret is a central animal model for development because of its early parturition. To date, most
61 visual development research in ferrets has focused exclusively on early visual stages. Here, we use
62 behavioral experiments to demonstrate that adult ferrets are capable of visual motion and form
63 integration. These complex visual functions are usually associated with higher-level visual areas in
64 monkeys and ferrets. We similarly observed good agreement between the motion integration

65 performance of neurons in PSS, a higher-level motion area in the ferret, and the behaviorally measured
66 motion integration capacity. Our experiments in the adult ferret demonstrate that the ferret is a viable
67 model for higher-level vision research, which provides exciting opportunities for developmental
68 research in this species.

69

70 **Introduction**

71 Because of their early parturition, ferrets are uniquely suited for developmental research. Indeed,
72 research in ferrets has contributed significantly to our understanding of the development of early visual
73 stages (Sharma and Sur, 2014). In contrast, higher-level visual areas have received little attention in this
74 species, even in adult animals. Behaviorally, ferrets have been shown to be capable of basic object
75 discrimination and motion detection tasks (Doty et al., 1967; Hupfeld et al., 2006). Anatomically, ferrets
76 have a relatively large visual system with about 19 areas (Homman-Ludiye et al., 2010), suggesting
77 extensive processing of visual information beyond primary visual cortex. Consistent with this notion, we
78 have recently demonstrated that one of these areas – area PSS (Philipp et al., 2006) – can be considered
79 a higher-level motion area comparable to primate MT (Lempel and Nielsen, 2019). These findings
80 suggest the feasibility of studying higher-level vision in ferrets, which would significantly enhance our
81 ability to investigate its development. To further establish higher-level vision research in ferrets, we
82 addressed two central aspects here: First, we used behavioral experiments to investigate whether
83 ferrets are able to perceptually integrate motion and form signals, functions that are usually associated
84 with higher-level visual areas (Ungerleider and Pasternak, 2004). Second, we tested whether PSS
85 responses are consistent with the behaviorally observed motion integration.

86 Following established methods, we tested behavioral and neural motion integration using RDK
87 (Figure 1). These stimuli consist of randomly placed dots, each of which can either move in a global
88 direction (signal dots), or in a randomly chosen alternate direction (noise dots). Integration over the

89 signal dots results in the perception of a coherently moving pattern, the strength of which depends on
90 the ratio of signal and noise dots (the so-called coherence level). Form integration was tested with a
91 very similar stimulus, static Glass patterns (Glass, 1969; Glass and Pérez, 1973). These patterns are
92 constructed from randomly distributed dot pairs (Figure 1). For signal dot pairs, the axis connecting the
93 two dots is oriented along a set orientation; noise pairs have a random orientation. Integration across
94 signal pairs then reveals a global pattern, with a strength that is again determined by the coherence
95 level.

96 We chose RDK and Glass patterns because they complement each other well: Processing of complex
97 motion and form information has been associated with different visual streams in non-human primates
98 and humans (Ungerleider and Pasternak, 2004). Yet, both stimulus types are constructed from the same
99 elements, and can be used for quantitative measurements of integration thresholds in a highly
100 comparable manner. In addition, both RDK and Glass patterns have been used to study the development
101 of motion and form vision in monkeys and humans (for reviews, see Grinter et al., 2010; Kiorpes, 2016;
102 Maurer and Lewis, 2018). Testing ferrets on RDK and Glass patterns therefore not only allows a
103 comparison of their motion and form vision capabilities, but also provides a useful starting point for
104 future developmental research.

105 Since very few visual behavioral experiments have been performed in ferrets (Doty et al., 1967;
106 Hollensteiner, 2015; Hupfeld et al., 2006, 2007; von Melchner et al., 2000; Pollard et al., 1967;
107 Pontenagel and Schmidt, 1980), testing their motion and form integration capacities required the
108 development of appropriate behavioral paradigms. Here, we established a freely-moving paradigm and
109 a head-fixed paradigm with greater control over viewing conditions. Using these paradigms, we found
110 that ferrets show clear signs of motion and form integration. In general, ferrets were good subjects for
111 visual psychophysics, performing tasks with low lapse rates, and behavior that could be well described
112 by standard psychometric functions. Furthermore, we found behavioral limits of motion integration to

113 be in close agreement with limits imposed by responses of PSS neurons, consistent with an involvement
114 of higher-level visual areas in these tasks. In summary, our data establish the ferret as a viable animal
115 model for studying more complex visual processes like motion and form integration.

116

117 **Materials & Methods**

118 Animals

119 All procedures were conducted in accordance with guidelines of the National Institutes of Health and
120 were approved by the Animal Care and Use Committee (ACUC) at Johns Hopkins University. A total of six
121 adult female ferrets aged 5 - 50 months at the start of the experiments were used for the behavioral
122 experiments. Each ferret participated in 1 - 3 studies of 1 - 4 months each (see Table 1 for the tasks each
123 ferret participated in and their sequence). An additional three female ferrets and one male ferret aged 2
124 - 12 months were used for electrophysiology recordings. Our previous experiments have shown no
125 difference in PSS motion integration in this age group (Lempel and Nielsen, 2019).

126

127 Freely-moving behavior: Design

128 *Freely-moving setup*

129 The behavioral box used for freely-moving behavioral tasks measured 100 cm long x 70 cm wide x 60 cm
130 tall (Figure 1a). The walls and the floor of the box were painted black, and the box did not have a ceiling.
131 The behavior box was enclosed in its own room such that the ambient light and noise level could be
132 controlled. A webcam (Logitech) affixed above the box was used to observe the ferret while performing
133 the task. A cut-out within one of the short walls of the box accommodated a 24 inch VIEWPixx/3D
134 monitor (VPixx) for displaying visual stimuli (refresh rate 120 Hz). Museum glass (True Vue) was placed
135 directly in front of the monitor to protect the screen and minimize reflectance. All stimuli were
136 generated using PsychToolbox (Brainard, 1997; Kleiner, M et al., 2007; Pelli, 1997), and stimulus timing

137 and trial events were controlled by PLDAPS (Eastman, 2012). Two reward ports were positioned to the
138 left and right side of the screen, and a third reward port was positioned in the center of the wall
139 opposite the screen. Reward ports consisted of a metal spout used for reward delivery, surrounded by
140 an infrared (IR) beam emitter and detector (Medical Associates Inc.). Breaks in the IR beam were used to
141 detect port contacts. A fourth IR beam was installed to detect crossing the halfway point between the
142 rear reward point and the monitor. Solenoid valves (Parker Hannifin) were used to dispense water
143 reward.

144

145 *General task design*

146 All ferrets were trained on two-alternative forced-choice (2AFC) tasks. Preceding a given trial, a red LED
147 was illuminated above the response port opposite the screen, indicating the start of a new trial (see
148 Figure 1b for task sequence). Ferrets initiated a trial by activating this port. Trial initiation was rewarded
149 with a small water reward (~0.05 mL). A stimulus was presented on the monitor immediately after trial
150 initiation, independent of which direction the ferret was facing at the time. With the exception of one
151 RDK control experiment, all stimuli were shown on gray background (50 cd/m²). Each stimulus was
152 associated with one of the two response ports located on either side of the screen. If the ferret selected
153 the correct port, a high tone (1 s duration) was played through the VIEWPixx speakers and a water
154 reward (~0.2 mL) was dispensed. If the ferret selected the incorrect port, a low tone (1 s duration) was
155 played and no water was dispensed. After an incorrect choice, the ferret was required to activate the
156 correct response port before it could initiate the next trial. Activation of the correct port was rewarded
157 with a small amount of water (10 - 30% of the maximum possible reward size, dependent on the
158 complexity of the task and stage of training). If ferrets demonstrated a significant bias towards one
159 choice port, the amount of water reward dispensed at each port was varied by the experimenter until
160 the ferret sampled both ports evenly.

161 In general, ferrets performed one session per day for 30 - 45 minutes, or about 100 trials. We
162 imposed no constraints on reaction time (i.e., the time between trial initiation and response port
163 activation), other than ending trials during which the ferret failed to make a choice for a long time
164 (around 120 s), which generally tended to only occur at the end of a testing session when motivation
165 levels were low. Because it took the ferret some time to move between the two ends of the box, the
166 shortest reaction times were around 2 s. In general, reaction time was about 3 s. For all tasks, the
167 stimulus presentation was tied to the reaction time of the animal. More precisely, with the exception of
168 the acuity task, in which the stimulus was removed when the ferrets reached the half-way point
169 between both ends of the box, the stimulus remained visible until the ferret selected the correct port. In
170 a subset of experiments, we measured both the time of the first response and the time of the correct
171 response. On incorrect trials, the ferret took about 2 s to correct its choice, meaning that the stimulus
172 was presented for a total of about 5 s.

173

174 *Acuity task: Stimuli, task design, training and animal inclusion criteria*

175 Ferret acuity was assessed with an orientation discrimination task, using horizontal and vertical gratings
176 of different spatial frequencies and contrasts (Figure 1 c). The contrast of each grating was varied from
177 0.05 – 0.95 Michelson contrast, and gratings were equiluminant with the background. To limit the
178 effects of changing viewing distance on the spatial frequency of the stimulus, the stimulus was turned
179 off once the ferrets crossed the IR beam at the midpoint of the box. Measured from this point in the box
180 (50 cm from the screen), gratings had a diameter of 33 deg, and a spatial frequency between 0.09 and
181 0.35 cycles per deg (cpd). Horizontal and vertical gratings were paired with the left and right choice port,
182 respectively. The orientation, spatial frequency, contrast, and phase of the grating were varied
183 pseudorandomly across trials. Five ferrets (F0, F1, F2, F3, F4) were trained on this task. Two ferrets (F1,

184 F3) failed to perform the task above 70% correct at a spatial frequency of 0.35 cpd and were excluded
185 from further analysis.

186

187 *Motion integration task: Stimuli, task design, training and animal inclusion criteria*

188 Ferrets were trained to discriminate between full-screen RDK with global translational motion to the left
189 or right (Figure 1d). RDK remained on the screen for the entire duration between trial initiation and
190 triggering the correct response port. Stimulus metrics below are given from the back of the box (viewing
191 distance 1 m). RDK measured approximately 38 x 24 deg, and were composed of black and white dots
192 (diameter 1.5 deg) with a density of 0.12 dots/deg. Dot position and color were randomly initialized.
193 Dots were randomly chosen to be signal or noise dots. The coherence parameter determined the
194 percentage of signal dots on each trial, and ranged from 20% - 100%. Motion directions differed
195 between signal and noise dots, but all dots moved at the same speed (also called “Brownian motion”
196 noise; (Pilly and Seitz, 2009; Schütz et al., 2010)). More precisely, signal dots moved in the global
197 stimulus direction (left or right), and noise dots in a direction randomly drawn from a uniform
198 distribution of integers from 0 to 359 deg. On the first frame, each dot was assigned a randomly chosen
199 lifetime that could range from 1 to 240 frames. Lifetime was decreased by one every frame. When the
200 lifetime of a dot reached zero, the dot was probabilistically assigned to be a signal or noise dot according
201 to the coherence parameter, and given a new lifetime of 240 frames. At this time point, noise dots were
202 assigned new motion directions, drawn from the same uniform distribution as before. Dots that moved
203 off-screen were re-plotted in a random position on the side of the screen opposite their direction of
204 motion. This wrap-around was designed to maintain constant dot density. In addition, random
205 repositioning after wrap-around and variable dot lifetime limited the subject’s ability to infer the
206 direction of coherent motion from a single dot in isolation.

207 Prior to training on the full motion integration task, ferrets were trained to associate a 100%
 208 coherent stimulus moving towards the right with reward at the right port, and a leftwards moving
 209 stimulus with the left port. Once ferrets mastered this task (performance at or above 95% correct for at
 210 least two consecutive sessions), increasingly lower coherence levels were introduced systematically
 211 across days. Three ferrets (F0, F4 and F6) were trained in this manner, and all three successfully learned
 212 the task. After completion of training, psychometric motion integration functions were measured by
 213 varying coherence level and direction pseudorandomly from trial to trial. Dot speed was kept constant in
 214 each session. Different dot speeds were explored in different blocks of sessions (i.e. a new speed was
 215 tested after completion of tests with the previous one). Across blocks, speeds of 24 deg/s, 48 deg/s, and
 216 72 deg/s (measured from the back of the box) were tested.

217 We ran a number of control experiments on individual ferrets (one ferret per experiment). In the
 218 first (ferret F4), we tested the impact of speed more directly by fixing the coherence at 60%, and varying
 219 dot speed pseudorandomly from 6 – 144 deg/s. In a second control experiment (ferret F0), we
 220 investigated the impact of dot lifetime by randomly setting maximum dot lifetime to either 240 or 3
 221 frames on any given trial. In the third control experiment (ferret F6), we tested the influence of dot color
 222 by using only white dots on a black background.

223

224 *Form integration task: Stimuli, task design, training and animal inclusion criteria*

225 Ferrets were trained to discriminate static linear Glass patterns based on their orientation (horizontal or
 226 vertical). As for the RDK task, stimuli remained on the screen for the entire trial duration, and stimulus
 227 parameters are given from a position in the last quarter of the box, assuming that ferrets made their
 228 decision after having turned around from the initiation port (viewing distance 75 cm). Stimuli covered
 229 the entire extent of the screen (38 x 24 deg). Each stimulus was composed of 200 - 250 white dot pairs
 230 (dot diameter 0.7 deg), with a distance of 1.2 deg between the dots in a pair. The position of all dot pairs

231 was randomly initialized. At 100% coherence, all dot pairs were oriented either horizontally or vertically
232 to create the global percept of a linear pattern (Figure 1e). At lower coherences, dot pairs were
233 randomly assigned to be signal or noise pairs, with the percentage of signal pairs determined by the
234 coherence parameter. Noise pairs were assigned a random orientation drawn from a uniform
235 distribution of integers from 0 to 359 deg. Ferrets began training the task with fully coherent patterns
236 until performance was at or above 85% for two consecutive sessions. At this point, increasingly lower
237 coherence levels were gradually introduced. In the full task, coherence varied from 20% to 100%. Both
238 the coherence level and the orientation of the glass pattern varied pseudorandomly from trial to trial.
239 Two ferrets (F0, F6) were trained on this on this task, and learned it successfully.

240

241 ***Head-fixed behavior***

242 *Head-fixed setup*

243 The head-fixed setup consisted of a head-post holder, body holder, and reward delivery system (see
244 Figure 4a & b). The body holder was a custom-made plastic box with adjustable sides that ferrets could
245 comfortably fit in, but that restricted their body movements (28.5 cm long, 10 cm wide, 10 cm tall; see
246 Dobbins et al., 2007 for a similar design). The head-post holder allowed stabilization of the animal's
247 head by means of a head-post. This head-post was anchored in an acrylic cap attached to the skull with
248 screws, which was implanted in an aseptic procedure under isoflurane anesthesia. The head-post holder
249 height and position was custom to each ferret to ensure an ergonomic position.

250 The reward delivery system consisted of three spouts: two choice spouts, positioned 12 mm apart,
251 and a neutral central spout that could be used for trial initiation (see Marbach and Zador, 2017 for a
252 similar design for mice). The spouts were made from metal tubes (1 mm in diameter) bent into the
253 correct shape. Licks were detected as changes in capacitance using an Arduino Uno board (Arduino) and
254 the Arduino capacitive-sensing library. The spouts were electrically isolated from the rest of the setup.

Each spout was mounted onto a pneumatic cylinder (McMaster-Carr), which used compressed air to retract and propel the spouts. This allowed each spout to assume two positions, one close to the animal, and one out of reach. The two choice spouts were additionally mounted on small translation stages (Newport) to control the distance between spouts. Finally, all spouts, along with the pneumatic cylinders, were mounted on a larger translation stage (Newport) to customize the distance of the spouts relative to the ferret. Solenoid valves (Parker Hannifin) were used to dispense water reward.

Stimuli were shown on the same VIEWPixx/3D monitor used in the freely-moving setup, which was placed 45 cm in front of the head-fixed setup. Stimuli again were generated using the PsychToolbox, and presentation was controlled using PLDAPS. We did not monitor eye movements during task performance for the data presented in this paper.

Task design for head-fixed paradigm

Ferrets were acclimated to the setup by receiving free water reward from each of the spouts while being head restrained. They were also permitted to freely move in and around the setup while the spouts were in motion to get comfortable with the noise of the gas pistons. This acclimation period lasted about three days. During this time, the position of the head-post holder and the spouts (relative to the ferret) were adjusted to optimize each animal's position and access to the spouts.

Each training session was preceded by a short calibration phase (20 trials) during which the ferret was presented with a single choice spout at a time and no visual stimulus. This calibration period served to ensure that both choice spouts were treated equally by the ferret, which helped to lower response biases. How the ferret valued each spout was estimated by the lick frequency on that spout. The head-post position and the amount of water delivered on each spout were adjusted until the ferret demonstrated approximately equal lick frequency on each spout.

Two ferrets were trained on a head-fixed 2AFC task using RDK generated identically to the freely-moving paradigm. As before, RDK could move horizontally to the left or right, and ferrets had to respond to each motion direction by licking one of the two choice spouts. Each trial in the task began with an initiation phase (see below), followed by stimulus presentation (see Figure 4c for task sequence). Following a 200-300 ms delay, the two choice spouts were then moved close the animal, which had to lick one of them to indicate its choice. As for the freely-moving paradigm, no constraints were imposed on reaction time. In general, the first spout contact occurred after about 650 ms from stimulus onset (i.e., within 250 to 350 ms from spout availability). If the ferret made the correct choice, the incorrect spout was retracted, and the ferret collected the full possible reward (~ 0.15 mL) from the correct spout. Instead of delivering the entire amount of water at once, we divided it into a series of smaller rewards (~30 μ L per lick), and delivered the entire amount over a series of licks. The total amount of water per correct trial was controlled by limiting how long the spout was available to the ferret (1.5 s, or about 5 licks). We chose this reward strategy because ferrets tended to spill less of the smaller drops, allowing better control over reward amounts per trial. If the ferret selected the incorrect spout, it was immediately retracted, and the ferret had to correct its choice by licking the correct spout for a single drop of water (~30 μ L) before moving on to the next trial. A high tone was paired with correct choices, and a low tone was paired with incorrect choices. The stimulus remained on the screen until the ferret selected the correct spout (in general, it took ferrets an additional 1 s to correct an incorrect choice). If a ferret demonstrated a significant bias towards one response port, the amount of water reward dispensed at each port was varied by the experimenter until the ferret sampled both ports more evenly.

Trial initiation differed between the two ferrets. For F9, trials were passively initiated. After the inter-trial interval (ITI), the stimulus appeared on the screen and the two choice spouts were presented. For F8, trials were actively initiated. In this case, a white square (3 x 3 deg) was presented in the center of the screen after the ITI, and the central spout was moved forward. When licks were detected on this

302 spout, the trial began: The center spout was retracted, the stimulus appeared on the screen, and the
303 two choice spouts were presented. Licks on the center spout were rewarded with a small amount of
304 water (about 30 μ L, divided into 2 – 3 licks performed during 0.5 s).

305 Prior to testing animals on the full motion discrimination task, ferrets were trained to associate
306 100% coherent RDK moving towards the right with reward at the right spout, and leftward RDK with
307 reward at the left spout. Ferrets were introduced to this task by adding a fraction of instructive trials, in
308 which only the correct spout was presented. This fraction was manually reduced both within and across
309 sessions by the experimenter to maintain an overall minimum reward rate of 75 - 80%, which ensured a
310 high level of motivation to perform the task. Once ferrets performed the task at or above 90% correct
311 with no instructive trials, increasingly lower coherence levels were gradually introduced across days. The
312 full task used coherence levels from 20 - 100%. For F9, trials at 100% coherence were doubly
313 represented and instructed 50% of the time, which served to increase the overall reward rate and
314 maintain a higher motivation level. Therefore, the number of uninstructed trials at 100% coherence was
315 the same as the number of trials at every other coherence level, and the overall fraction of instructive
316 trials was ~14%. Instructed trials were excluded from further analysis. For F8, no trials at any coherence
317 level were instructed, and all coherence levels were presented equally often. Coherence level and
318 direction of motion varied pseudorandomly from trial to trial. Dot speed was fixed at 72 deg/s. The total
319 number of trials per session that ferrets performed in the head-fixed setup was generally higher than
320 the freely-moving behavior, but also more variable per ferret. In general (including initial training
321 sessions at 100% coherence only), F8 would perform about 200 - 500 trials, while F9 would perform
322 about 100 - 150 trials.

323

324 Behavioral data: Analysis and statistics

325 All data analysis was performed in MATLAB (The Mathworks). Data was concatenated across sessions for
326 which the ferret performed at least 70 trials in the freely-moving paradigm and at least 100 trials in the
327 head-fixed paradigm (see Tables 2 and 3 for a summary of number of trials and sessions for each
328 analysis). This criterion was imposed because behavioral training sessions in which ferrets performed
329 fewer trials were indicative of decreased motivation and attention. Such training sessions were rare, and
330 nearly always followed a break in behavioral training for a week or more. In one data set for the freely-
331 moving motion integration paradigm, a session in which the ferret performed 187 trials was excluded.
332 Of the six sessions performed at the specified parameters for this task, the other five sessions had a
333 mean of 100 trials with a standard error of 7. We therefore felt that the session with 187 trials was an
334 outlier that exerted undue influence on the fit of the psychometric function.

335 We characterized behavior using three measures, a sided threshold Δ and thresholds corresponding
336 to 75% and 82% correct. To compute Δ , we first computed signed contrast or signed coherence values,
337 where negative values indicated conditions assigned to the left port, and positive values conditions
338 assigned to the right port. We then determined the fraction of right port responses for each condition.
339 The resulting psychometric curves were fit with a cumulative Gaussian using the Palamedes toolbox for
340 MATLAB (Prins and Kingdom, 2018). Separate lapse rates were fit for left and right responses. 95%
341 confidence intervals for psychometric curves were computed for a binomial using the Clopper-Pearson
342 method (Clopper and Pearson, 1934). Finally, Δ was defined as the change in contrast or coherence
343 required to increase the probability of a right choice from 50% to 68% of the maximum fraction of right
344 responses (Busse et al., 2011). To compute thresholds based on percent correct responses, we first
345 averaged performance across the two sides. The resulting data were then fit with a cumulative Weibull
346 function using the Palamedes toolbox, and thresholds determined as the contrast or coherence levels
347 required to reach a performance of 75% or 82% correct.

348 Contrast sensitivity curves were fit using a double exponential of the form $k_s (\omega \cdot k_\omega)^\alpha \exp(-\beta \cdot \omega \cdot k_\omega)$,
 349 where ω is the spatial frequency (Kiper and Kiorpes, 1994). The parameters k_ω and k_s capture shifts
 350 along the frequency and sensitivity axes, respectively, while α and β capture the steepness of the low
 351 and high frequency portions of the curve. This sensitivity curve was fit using an `fminsearch` algorithm in
 352 MATLAB. Error bars for sensitivity estimates were calculated by parametrically bootstrapping the data
 353 1000 times, and fitting these bootstraps with psychometric functions to create a distribution of
 354 sensitivity estimates (Efron and Tibshirani, 1986). These represent 68% confidence intervals, or
 355 approximately one standard deviation from the mean.

356 The fidelity of the fit of a psychometric function was evaluated in two ways. First, the deviance of
 357 the fit was computed (Wichmann and Hill, 2001), which is defined as the extent to which the fit deviates
 358 from a saturated model in which there are no residual errors between the observed data and the fit.
 359 This tests how likely the fit is given the data. By convention, fits with deviance with significance less than
 360 0.05 are rejected. The deviance and its significance were computed using the Palamedes goodness-of-fit
 361 function with 1000 simulations. Second, the mean squared error (MSE) between the model and the data
 362 was also computed.

363 To evaluate the statistical significance of differences between psychometric curves, likelihood ratios
 364 were computed of the form $\lambda = (L(\text{data} \mid \text{single curve}) / L(\text{data} \mid \text{independent curves}))$ (Britten et al.,
 365 1992; Hoel, P. et al., 1971). $-2\ln(\lambda)$ is distributed as chi-squared with degrees of freedom equal to the
 366 difference in dimensionality between the lesser and fuller model (Wilk's theorem). Differences between
 367 two thresholds were tested for significance by parametrically bootstrapping the data sets 1000 times,
 368 and generating a distribution of thresholds for each. A Welch's t-test was then used to determine
 369 whether the bootstrapped threshold distributions were significantly different. On the other hand, to
 370 test whether two thresholds were equivalent each dataset was bootstrapped 1000 times, and a
 371 distribution of the differences in the threshold values was generated. The equivalence bound was set to

372 2.5%, and the probability of threshold differences falling within this equivalence bound was derived
373 from the difference distribution. This test for equivalence (TOST) yielded the p-value (Walker and
374 Nowacki, 2011). Tests for equivalence were always performed on data from the same animal on the
375 same task with two different stimulus conditions, and were only performed when the difference
376 between psychometric curves was not statistically significant.

377

378 ***Electrophysiology***

379 *Animal preparation and recordings*

380 The electrophysiology experiments followed established methods detailed previously (Lempel and
381 Nielsen, 2019). Briefly, experiments were performed in animals anesthetized with isoflurane (during
382 surgical procedures: 2 – 3%, during recording: 0.5 – 1.5%). Animals were paralyzed with pancuronium
383 (0.15 mg/kg/hr) to prevent eye movements during recordings. A number of vital parameters (EtCO₂,
384 SPO₂, heart rate and EEG) were monitored continuously to maintain animals at appropriate anesthetic
385 depths. Neural signals were detected using either custom-built tetrodes or 64-channel silicon
386 microprobes (Masmanides lab, UCLA). Tetrodes were made using 12 μ m nichrome wire (California Fine
387 Wire Company), and were plated using a gold solution (Sifco ASC) to reach final impedances of 150-500
388 k Ω . Silicon probes were gold-plated to reach final impedances of 150-300 k Ω . Signals were amplified and
389 recorded using either a CerePlex Direct amplifier (Blackrock Microsystems) or a RHD2000 amplifier
390 (intan Technologies). Raw data was acquired at 30 kHz and filtered between 250 Hz and 5 kHz. A total of
391 10 penetrations were made across the 3 animals. The number of cells recorded concurrently (that were
392 included in the analysis as significantly responsive and direction selective; see below) ranged between 1
393 and 4 cells. Of the 34 neurons included in the final analysis (see below), 7 were recorded using the
394 multichannel probes; the rest were recorded using tetrodes.

395

396 *Stimuli*

397 Visual stimuli were displayed on a gamma corrected 24" LCD monitor with a refresh rate of 120 Hz. The
398 monitor was placed 25 – 35 cm in front of the ferret. RDK stimuli consisted of white dots shown on a
399 black background. Otherwise, they were constructed identically to the behavioral experiments. Dot
400 speed was fixed at 48 deg/s. For the tetrode recordings, we manually determined the preferred
401 direction of the neuron under study in an initial experiment. The main experiment then consisted of RDK
402 moving either in the neuron's preferred direction or in the opposite (null) direction. For multichannel
403 probe recordings, we initially determined the preferred direction of a selected neuron, and then used
404 this direction and its opposite for the RDK. In addition to the initially selected neuron, other neurons
405 that also strongly responded to the chosen RDK direction and that passed our selection criteria (see
406 below) were also included in the analysis. In 1 multichannel recording experiment, we repeated the
407 experiment with a different set of directions to drive a second group of cells with very different stimulus
408 preferences, making sure that nonoverlapping sets of neurons resulted from these experiments.
409 Coherences were varied from 10 - 100%, and each coherence level and direction was repeated 20 times
410 in a pseudo-random sequence. 20 blank trials were randomly interleaved throughout the experiment.
411 Each RDK trial began with a static presentation of the first frame of the RDK for 2 s to control for
412 responses to luminance changes. Dots then moved for 1 s, before presenting the last frame statically for
413 0.5 s. A blank black screen was shown between trials.

414

415 *Data analysis and statistics*

416 Single unit isolation was performed off-line using custom MATLAB software. A spike detection threshold
417 was set manually for each recording. Isolation was then based on multiple spike waveform
418 characteristics (e.g., spike amplitude peak, area under the waveform, repolarization phase slope etc.)
419 recorded on the four tetrode channels or on neighboring channels of the silicon probe (see Figure 7b for

420 an example). Quality of isolation was confirmed by inter-spike interval (ISI) analysis. Units that displayed
421 ISIs below 1.2 ms were excluded.

422 Identified single units had to pass two criteria to be included in further analyses. First, they had to
423 be responsive, as indicated by a significant difference in responses to the preferred direction and blanks
424 (student's t-test, $p < 0.01$), as well as a response rate of at least 6 spikes/s for the best stimulus. Second,
425 they had to be direction selective, quantified as a significant difference in responses between preferred
426 and null direction (student's t-test, $p < 0.01$). 43 of 72 recorded neurons passed the responsiveness test,
427 and 37 of the 43 neurons (86%) were considered direction selective.

428 We used established approaches to compute neurometric curves (Britten et al., 1992; Green and
429 Swets, 1966). For a given single unit, the distributions of responses to its preferred and null direction
430 were computed at each coherence level. Here, a response is defined as the number of spikes during the
431 1 s presentation of the moving RDK. A receiver operating characteristic (ROC) curve was then generated
432 for each coherence level by setting a threshold, and determining the probabilities that the preferred or
433 null direction elicited a response exceeding the threshold. Thresholds could range from 0 to each cell's
434 maximum response and were increased in steps of 1 impulse (similar to Britten et al., 1992). The area
435 under the ROC curve (aROC) for a given coherence was taken to be a proxy for the fraction correct that
436 would be obtained from listening to the neuron's responses, and used to construct a neurometric
437 function for each neuron. Finally, a cumulative Weibull function was fit to the estimated fraction correct
438 at each coherence level using the Palamedes toolbox. Thresholds were estimated from each of these
439 curves using a criterion of 75% correct. 1 neuron was excluded from further analysis because the
440 Weibull function fit failed to converge, and 2 additional neurons were excluded because their aROC at
441 100% coherence was below 0.75. This resulted in a total of 34 neurons for the full analysis.

442

443 Results

444 **Behavioral estimates of visual acuity**

445 Most of the existing studies on ferret visual behavior tested the animals in setups in which they could
446 move freely and earn food or water reward for performing a particular action (such as opening a door)
447 in response to a visual stimulus (e.g., Doty et al., 1967; Hupfeld et al., 2006; von Melchner et al., 2000;
448 Pollard et al., 1967; Pontenagel and Schmidt, 1980). These behavioral paradigms have the advantage of
449 closely mimicking natural foraging behavior. They also do not require the cranial implants necessary for
450 head-fixed paradigms. Thus, they lend themselves to expedient testing of large cohorts of animals, as
451 may be required by some developmental studies. We therefore decided to first implement a similar
452 freely-moving testing paradigm.

453 Our behavioral setup was designed for 2AFC discrimination tasks. It consisted of an open box with a
454 screen placed on one wall for visual stimulus presentation (Figure 1a). This screen was flanked by two
455 choice ports, each consisting of an IR beam emitter and detector surrounding a water spout. Every visual
456 stimulus was associated with one of the choice ports. A similarly constructed trial initiation port was
457 placed in the middle of the wall opposite the screen. The animal initiated each trial by breaking the
458 beam in this port (see Figure 1b for task sequence). This triggered stimulus presentation, and was
459 rewarded with a small amount of water from the trial initiation port. The animal then had to respond to
460 the stimulus by crossing the box, and selecting one of the two choice ports. Selection of the correct port
461 resulted in the delivery of a water reward, removal of the stimulus (depending on the task), and ending
462 of the trial. If the animal instead chose the incorrect port, it could not advance to the next trial before
463 activating the correct port. Once the animal corrected its choice, a small water reward (1/10 of the full
464 amount) was delivered to maintain engagement in the task. Requiring ferrets to choose the correct port
465 in order to complete the trial was essential in encouraging an even sampling of both ports early in
466 learning, and was useful in preventing biased behavior during all testing stages.

467 We first used this setup to estimate the ferret's visual acuity behaviorally, a necessary prerequisite
468 for determining appropriate stimulus parameters for the experiments to follow. We therefore trained
469 ferrets to discriminate horizontal from vertical gratings (Figure 1c), and varied grating contrast and
470 spatial frequency across trials (contrast range: 0.05 – 0.95 Michelson contrast, spatial frequency range:
471 0.09 – 0.35 cpd). To limit changes in spatial frequency induced by changes in viewing distance, stimuli
472 were only shown until the ferret crossed an IR beam halfway between the trial initiation port and the
473 screen. The spatial frequency values given above are calculated from this point.

474 Visual acuity was determined for 3 adult ferrets (see Methods for animal selection criteria). On
475 average, the animals performed 103 trials per session (SEM: 4 trials) and achieved good performance for
476 the easiest conditions (see Table 1 – 3 for training history for individual animals, trial and session
477 numbers, and statistics per animal). For the optimal spatial frequency (0.18 cpd) and the highest
478 contrast, ferrets averaged 90% correct (SEM: 5.25% correct). In addition, their performance depended
479 predictably on stimulus contrast and spatial frequency. This is clearly demonstrated by computing
480 performance as a function of grating contrast for each spatial frequency (see Figure 2a for an example
481 ferret): For all spatial frequencies, performance was close to chance level for low contrasts, but
482 improved rapidly with increases in contrast. For further analysis, we captured the dependency of
483 performance on contrast at each spatial frequency in the following way: We first computed
484 performance as a function of grating contrast for each spatial frequency individually. To better account
485 for potential response biases, performance was quantified as the fraction of vertical responses, and
486 contrasts were expressed as 'sided' contrasts, with -1 indicating a full contrast horizontal grating, and +1
487 a full contrast vertical grating. The resulting data were fit with a cumulative Gaussian to generate a
488 psychometric function per spatial frequency. We then determined the 'sided' contrast threshold Δ for
489 each psychometric function, defined as the contrast increment required to go from 50% vertical
490 responses to 68% of the maximum fraction of vertical responses (i.e. to 68% of 1 minus the lapse rate).

491 Finally, the contrast sensitivity for a spatial frequency was defined as the inverse of Δ . The same
 492 approach has previously been used to evaluate acuity in mice (Busse et al., 2011).

493 In general, fits were based on aggregating behavior across multiple sessions for each ferret (N=14
 494 +/- 2) to improve the estimation of contrast sensitivity. However, we verified in one ferret (F4) that
 495 performance was indeed consistent across days. For this animal, we fit data of individual sessions
 496 performed at a spatial frequency of 0.18 cpd, and determined a sided coherence threshold Δ for each
 497 session. These data confirmed that thresholds were highly similar across sessions (Figure 2b, standard
 498 deviation of Δ : 1.28%).

499 Finally, we used the collected data to compute a contrast sensitivity curve for each ferret. To this
 500 end, contrast sensitivity as a function of spatial frequency was fit with a double-exponential function
 501 (see Methods for details). The fit to the contrast sensitivity curve could then be used to determine two
 502 measures for every ferret: First, peak frequency, which corresponded to the spatial frequency with
 503 maximal contrast sensitivity. Second, cutoff frequency (also called maximum visual acuity), which
 504 corresponded to the spatial frequency with a contrast sensitivity of 1, and was determined by
 505 extrapolating the fit. Contrast sensitivity curves were highly similar across ferrets (Figure 2c). They
 506 revealed an average peak spatial frequency of 0.18 cpd (SEM: 0.010 cpd), and average cutoff frequency
 507 of 0.65 cpd (SEM: 0.029 cpd).

508 Our behavioral estimates of contrast sensitivity and acuity are in good agreement with existing data
 509 on spatial frequency tuning in ferret area 17 (Baker et al., 1998). The optimal spatial frequencies for area
 510 17 neurons range from about 0.1 to 0.5 cpd, with a geometric mean of 0.25 cpd. Furthermore, neurons
 511 with the highest spatial frequency preference have an average bandwidth of 1 octave. Thus, not only is
 512 the behaviorally measured peak sensitivity close to the average optimal spatial frequency for area 17,
 513 the cutoff frequency also falls within the range of spatial frequencies that can elicit responses in area 17.
 514 While there are limitations to estimating acuity based on freely-moving behavior, the good match

515 between behavior and neural data strongly supports our measurements. We therefore used these data
516 as a basis for selecting stimulus parameters for the following experiments, in particular the size of dots
517 in RDK and Glass patterns.

518

519 **Measurements of motion integration in freely-moving ferrets**

520 Based on the success of the acuity experiment, we used the same freely-moving paradigm to probe
521 higher-level motion processing by testing whether ferrets were capable of motion integration. RDK
522 (Figure 1d) have become the standard stimulus to assess visual motion integration performance, as they
523 can be constructed so that integration across multiple dots is required for perceiving a global direction
524 signal. Here, 3 ferrets were trained to discriminate RDK based on their global direction (left versus right)
525 at a dot speed of 48 deg/s. Ferrets were introduced to this task at 100% coherence (i.e. with all dots
526 moving in the global direction), and continued with 100% coherent motion until they performed at 80%
527 correct or above. All ferrets demonstrated rapid learning, and reached criterion at 100% coherence
528 within 3 - 5 sessions.

529 At full coherence, the direction discrimination task could theoretically be solved by attending to a
530 single dot. Lower coherences require integration of motion information across dots, and therefore more
531 accurately reflect motion integration capabilities. In addition, systematic changes in coherence levels
532 allow threshold measurements, and thereby a quantitative assessment of motion integration
533 capabilities. For this reason, we gradually introduced RDK with lower coherence once criterion
534 performance was reached for the full coherence. After 3 – 5 additional sessions, ferrets performed the
535 RDK task across a range of coherence levels (20 - 100% coherence). For the remaining analysis, only data
536 from sessions in which the ferrets were assessed on the full range of coherences were included (3-12
537 sessions per animal).

538 In general, ferrets exhibited excellent performance on the easiest direction discrimination
 539 conditions: They performed on average at 98% correct for 100% coherent motion (SEM: 0.21%). These
 540 low lapse rates show that ferrets not only mastered the task, but that the behavior was under tight
 541 stimulus control. Consistent with a performance that is mainly driven by the information present in the
 542 motion stimulus, each ferret's performance systematically depended on the coherence level. Once
 543 again, performance was quantified by computing a sided performance measure to appropriately address
 544 any response bias. More precisely, for each ferret we computed the fraction of right motion responses
 545 as a function of a sided coherence measure (-100%: full coherence, direction left; +100%: full coherence,
 546 direction right). These data were then fit with a cumulative Gaussian (Figure 3a). Data from all ferrets
 547 could be fit well: No fits exhibited significant deviance from a saturated model (F0: deviance = 7.04, $p =$
 548 .143, F4: deviance = 10.02, $p = .199$, F6: deviance = 9.19, $p = 0.128$, see Methods), and on average, fits
 549 had a MSE of 2.34 (SEM: 0.078).

550 Motion integration capacity was then quantified based on the fits by computing a sided coherence
 551 threshold Δ (see Table 3 for data from individual ferrets and alternate threshold measures). Analogous
 552 to the computation of the contrast threshold, we defined Δ as the increase in coherence required to
 553 change the fraction of right responses from 50% to 68% of the maximum. This analysis yielded an
 554 average Δ across ferrets of 17.62% (SEM: 1.30%). Note, however, that these thresholds were
 555 determined after a limited number of sessions to quantify the general motion integration capacity of
 556 adult ferrets. Thresholds could be improved significantly by additional training (Figure 3b): We
 557 continued to train F4 after the initial threshold measurement. A re-evaluation after 11 additional
 558 sessions resulted in a sided coherence threshold Δ of 9.44%, significantly lower than the initial value of
 559 15.01% (log-likelihood ratio test, $-2 \cdot \ln(\lambda) = 15.83$, degrees of freedom = 2, $p = 3.6576 \times 10^{-4}$).

560 Performance on the RDK task might be expected to depend on dot speed. We therefore measured
 561 motion integration thresholds at 3 speeds: 24 deg/s, 48 deg/s, and 72 deg/s. No clear effect of speed on

562 threshold was observed over this range (Figure 3c). To investigate further, the performance of one ferret
563 was evaluated at a fixed dot coherence (60%) and variable speed per trial (6 - 144 deg/s). In agreement
564 with the larger data set, the ferret's performance in the control experiment was largely independent of
565 speed (Figure 3d). For speeds larger than 7.22 deg/s, the ferret performed above 75% correct, and
566 performance was at or above 95% correct for speeds above 24 deg/s.

567 Finally, we performed two control experiments to test whether task performance was indeed due to
568 integration of signals across dots, and not other stimulus factors. In the first control experiment, we
569 tested the impact of dot lifetime, which determined how long each individual dot could remain a signal
570 dot. Long lifetimes might allow a ferret to solve the task based on the trajectory of a single dot, rather
571 than through integration. Thus, in the control experiment we randomly set lifetime to either 25 ms or 2
572 s at the beginning of every trial. Performance on the task (Figure 3e) did not differ significantly between
573 the two lifetime conditions (log-likelihood ratio test, $-2 \ln(\lambda) = 3.07$, degrees of freedom = 2, $p = .2156$),
574 and Δ values for each condition were equivalent within 2.5% of each other (TOST, $p = 10^{-3}$), indicating
575 that at least the ferret used in the control experiment was not following single dots to perform the task.
576 In a second control experiment, we tested the impact of dot color. In the RDK experiments described so
577 far, 50% of the dots were black and 50% white to provide some stimulus contrast to the animals (shown
578 against a gray background). To rule out any effects of this color choice, we tested performance for RDK
579 constructed from white dots only, shown on a black background (Figure 3f). Again, the change in
580 stimulus parameter did not affect performance in the control experiment (log-likelihood ratio test, -
581 $2 \ln(\lambda) = 0.945$, degrees of freedom = 2, $p = 0.6233$; Δ between conditions equivalent within 2.5%,
582 TOST, $p = 0$). In summary, our experiments demonstrate a clear capacity for motion integration in
583 ferrets.

584

585 **Tests of motion integration using a head-fixed paradigm**

586 The freely-moving behavioral paradigm used so far excels in its ease of implementation. Ferrets
587 generally learned quickly using this paradigm, and the results of the first two experiments confirm its
588 suitability for psychophysical experiments. The main disadvantage of freely-moving behavior is a limited
589 control over viewing distance and head position. Variable viewing distances and head positions
590 complicate accurate estimates of how stimulus parameters such as stimulus speed, size, and spatial
591 frequency influence task performance. Furthermore, freely-moving behavior does not lend itself as
592 easily to simultaneous neural recordings, in particular using optical methods. For these reasons, we also
593 developed a head-fixed behavioral paradigm. We then used this paradigm to measure motion
594 integration performance in two additional ferrets, which allowed a direct comparison of behavior in the
595 two paradigms.

596 The head-fixed setup consisted of a head-post holder, a body holder, and three independently
597 movable water spouts for reward delivery (Figure 4a & b). Licks on the water spouts could be detected
598 as changes in spout capacitance (see Methods for details). A screen for visual stimulus display was
599 placed 42 cm in front of this setup. The head-post holder allowed fixation of the head by means of an
600 implanted head post, while the body holder limited movements by the rest of the body. A similar
601 configuration has been used for auditory studies in ferrets (e.g., Dobbins et al., 2007; Fritz et al., 2003).
602 At the beginning of training, the relative positioning of head-post holder and body holder were
603 customized for each ferret to ensure a comfortable posture, and the animals were slowly acclimated to
604 the setup (see Methods). The relative position of the water spouts was optimized such that the animal
605 could lick them easily but distinctly: in other words, the animal could not contact more than one spout
606 at the same time.

607 In order to mimic the structure of the freely moving behavioral paradigm, the central spout was
608 designated as the trial initiation spout, while the two peripheral spouts were designated as choice
609 spouts. Each spout had two positions: a retracted position, where the animal could not reach the spout,

610 and a forward position, where the animal could lick the spout easily. Usually, ferrets did not lick while
611 the spouts were retracted. Thus, the potential of motion artifacts throughout the trial – which could
612 pose problems for combined behavioral and recording experiments – could be further limited by
613 controlling the availability of the water spouts. A similar three-spout configuration, albeit with stationary
614 spouts, has been used in mice (Marbach and Zador, 2017).

615 The head-fixed 2AFC task used the following design (Figure 4c): During the ITI, all spouts were in the
616 retracted position. After the ITI and a trial initiation phase (see below), a visual stimulus was presented
617 on the screen. Following a brief delay, the two peripheral choice spouts were then moved forward, and
618 the ferret had to respond to the visual stimulus by licking one of them. As in the freely-moving
619 paradigm, we implemented a task design that forced sampling of both ports: In the case of a correct
620 response, water was delivered as soon as the ferret contacted the spout. At the same time, the second
621 spout was retracted. If the ferret instead chose the incorrect spout first, this spout was immediately
622 retracted without reward. The ferret then had to correct its choice by contacting the remaining correct
623 spout – rewarded with a much smaller amount of water – to end the trial. At this point, the correct
624 spout was also retracted.

625 We explored two different trial initiation options with the two ferrets. In one ferret (F9), trials were
626 passively initiated. For this animal, each trial began automatically after a fixed ITI by presenting a white
627 square on the screen, which served to alert the animal to the upcoming stimulus presentation. In this
628 design, the central spout was not used. In the other ferret (F8), we explored an active trial initiation.
629 After the ITI elapsed, a white square again was presented on the screen. At the same time, the central
630 spout was moved forward. The animal was required to lick this spout (rewarded with a small amount of
631 water) to fully initiate the trial. The spout was then retracted, and the visual stimulus presented after a
632 brief delay. While this full three-spout version of the task might be more challenging to learn, it offers

633 the advantage of starting each trial with a central licking position, which could help reduce biases for the
 634 subsequent response choice.

635 As before, ferrets were initially trained on the RDK direction discrimination using stimuli with 100%
 636 coherence (dot speed 72 deg/s). Both ferrets learned the task, and participated well. F9 performed at
 637 80% correct or above within 1 week of training, while F8 reached the same criterion within 3 weeks of
 638 training. F9 performed 142 trials per session on average (SEM: 14 trials), and F8 performed 469 trials on
 639 average (SEM: 15 trials). The data collected from the head-fixed task exhibited many of the same
 640 properties observed for the freely-moving paradigm (Figure 5). First, ferrets again performed the task
 641 with low lapse rates (3.81% +/- 1.96%, mean and SEM), comparable to the lapse rates for freely-moving
 642 animals (for 72 deg/s: 0.91% +/- 0.14%, mean and SEM). Thus, despite the fact that the different setups
 643 might have been expected to produce differences in motivational state (such as the overall willingness
 644 to perform the task, the subjective cost incurred by an error, etc.), performance was under similarly
 645 strong stimulus control in both paradigms. Second, psychometric functions were again well described by
 646 a cumulative Gaussian (F9: deviance = 1.76, $p = 0.802$, MSE = 0.25, F8: deviance = 3.69, $p = 0.760$, MSE =
 647 0.67). Sided coherence thresholds Δ based on these fits were 18.36% for F9 and 28.35% for F8. This
 648 places F9's performance well within the range of Δ values observed for the same speed in the freely-
 649 moving paradigm (12.79% - 20.06%), while F8's performance was somewhat worse. Note, however, that
 650 since F8 performed so many trials per session, we used only 2 sessions to compute Δ for this ferret. For
 651 all other ferrets, 4 – 12 sessions were used to determine the threshold. It is possible that extra training
 652 provided by additional sessions would have lowered thresholds for F8 to be more similar to the other
 653 ferrets.

654 The speed of task learning, low lapse rates, and fidelity of psychometric function fits demonstrate
 655 that a head-fixed 2AFC task design can be used for visual psychophysics in ferrets, thus opening the door
 656 for future work combining neural recordings with visual tasks in ferrets. Since no major differences were

657 observed between the three- and two-spout versions of the task, both are viable designs. Moreover, the
658 general agreement of thresholds across paradigms suggests that they may be used to complement one
659 another.

660

661 **Form integration capacity of adult ferrets**

662 The experiments described above demonstrate clearly that ferrets are capable of complex motion
663 vision. Another important aspect of higher-level vision – at least in primates – is the ability to process
664 form information, a function that is usually associated with different visual areas than processing of
665 motion information (Ungerleider and Pasternak, 2004). While it is unclear whether the same holds for
666 ferrets, at least their basic capacity to perform tasks requiring general form discrimination has been
667 demonstrated (Doty et al., 1967; Pontenagel and Schmidt, 1980). Rather than investigating the most
668 complex aspects of form vision (such as object recognition), we decided to study form vision at a
669 comparable level of complexity to the RDK motion integration task. To this end, we chose Glass patterns
670 (Glass, 1969; Glass and Pérez, 1973). In addition to consisting of similar elements as the RDK, Glass
671 patterns offer the advantage of allowing measurements of form integration thresholds in a comparable
672 manner to the motion integration thresholds. For these reasons, they have been used to assess the
673 development of sensitivity to global form sensitivity in humans and monkeys, and to compare it to the
674 development of sensitivity to global motion (Kiorpes et al., 2012; Lewis et al., 2004). Glass patterns can
675 be constructed to yield different global patterns, including concentric, radial or linear forms. Here, we
676 chose linear Glass patterns (Figure 1e), because they allowed us to continue to use a 2AFC task very
677 similar to the task used for the RDK.

678 Two ferrets were trained to discriminate horizontal from vertical Glass patterns. All tests used
679 the freely-moving paradigm because of its easier implementation. As for the RDK, Glass patterns were
680 introduced at 100% coherence, and remained at this level until ferrets achieved a criterion performance

681 of 80% correct. Lower coherence levels were then gradually introduced in subsequent sessions. In the
 682 following analyses, data were limited to behavioral sessions that used the full range of coherences (20 -
 683 100%). Ferrets were able to learn the basic Glass pattern task (Figure 6), and achieved good
 684 performance on the easiest condition (F0: lapse rate = 91%, F6: lapse rate = 87%). Their overall
 685 behavioral data was once again well described by cumulative Gaussian functions (F0: deviance = .379, p
 686 = 0.774, MSE = 2.06; F6: deviance = 0.401, p = 0.5780, MSE = 1.31). Sided form coherence thresholds Δ
 687 were computed identically to the sided motion coherence thresholds to facilitate a comparison across
 688 tasks (see Table 3 for other thresholds). For F0, this analysis resulted in a threshold of Δ = 21.32%; the
 689 threshold for F6 was Δ = 23.25%. Both ferrets were previously tested on the freely-moving motion
 690 integration task, allowing a direct comparison of thresholds between the two tasks. For both ferrets,
 691 thresholds were significantly higher in the Glass pattern than the RDK task (F0: 2.38% difference in Δ
 692 between RDK at 48 deg/s and Glass pattern task, p = 7.919e-189, t = 32.77, df = 1998; F6: 4.34%
 693 difference in Δ , p = 7.169e-138, t = 27.08, df = 1998). This suggests that even though they were able to
 694 learn both tasks, the ferrets found the Glass pattern task more challenging than the RDK task. The
 695 increased difficulty may reflect genuine differences in processing of form versus motion information in
 696 ferrets. However, since both ferrets were trained on the motion before the form task, we can't rule out
 697 that the training sequence caused interference between the two tasks.

698

699 **Comparison of behavioral and neural motion integration limits**

700 The experiments described above were designed to test behaviorally whether ferrets are able to
 701 integrate motion and form information, functions that are associated with mid-level visual areas such as
 702 MT and V4 in the primate (Orban, 2008; Ungerleider and Pasternak, 2004). An important aspect of
 703 establishing higher-level vision research in ferrets will be to identify the areas supporting the more
 704 complex visual behavior we observed. Little is currently known about processing of form information in

705 ferret visual cortex outside of area 17 and 18. The same largely holds for motion processing. However,
 706 previous studies have identified one higher visual area involved in motion processing (Hupfeld et al.,
 707 2007; Philipp et al., 2006). This area – called PSS or PMLS – is located in the posterior bank of the
 708 suprasylvian sulcus (Figure 7a). Building on this finding, we recently demonstrated that PSS shows the
 709 same signatures of complex motion processing that are observed in primate MT (Lempel and Nielsen,
 710 2019). This includes a significant change in the degree of motion integration between area 17 and PSS:
 711 As in the primate motion pathway (Born and Bradley, 2005; Orban, 2008), motion processing in area 17
 712 is concerned with local motion signals, while PSS extracts integrated, global motion signals.

713 This provides the opportunity to test whether the behaviorally observed motion integration is
 714 consistent with limits imposed by neural activity in higher-level area PSS. Ultimately, the contribution of
 715 PSS to visual motion integration behavior will need to be addressed by recording and manipulating
 716 neural activity during the task. However, as a first step we compared behavioral thresholds with
 717 thresholds of PSS neurons recorded in a different group of animals during anesthetized experiments. In
 718 these experiments, we used tetrodes or multi-site silicon probes to isolate responses of individual PSS
 719 neurons. For each neuron, we first determined the preferred direction. We then collected responses to
 720 repeated presentations of RDK with varying coherence levels. RDK could move either in the neuron's
 721 preferred direction, or the opposite (null) direction at a fixed speed of 48 deg/s. These data allowed us
 722 to use a signal detection theory approach to determine the likelihood of correctly detecting the
 723 preferred direction based on the firing rates of the recorded neuron (Green and Swets, 1966). More
 724 precisely, the measured firing rate distributions for preferred and null direction were used to calculate
 725 ROC curves at each coherence (Figures 7b – 7c). The probability of correctly detecting motion in the
 726 preferred direction at a coherence level could then be estimated from the area under the corresponding
 727 ROC curve (aROC). aROC values need to reach reasonably high levels for the remainder of the analysis to
 728 be meaningful. Figure 7d therefore shows the area under the curve (aROC) at 100% coherence for 36

729 responsive and directionally selective neurons. To be included in further analysis, neurons were required
730 to reach a minimum aROC value of 0.75. 34 neurons remained after this step, and were each fit with a
731 Weibull function to capture the dependency of detection probability on coherence level (Figure 7e). This
732 neurometric function was used to estimate the integration threshold for each neuron as the coherence
733 required to reach 75% detection probability. A similar approach has been used previously to compare
734 neural responses in primate MT to behavioral motion integration performance (Britten et al., 1992).

735 Figure 7f plots the resulting distribution of PSS neurometric thresholds and the matching behavioral
736 thresholds collected from 3 ferrets tested on the same dot speed in the freely-moving paradigm. To
737 directly compare neural and behavioral results, we recomputed behavioral thresholds as the coherence
738 levels required to reach 75% correct, instead of the sided coherence threshold used earlier (see Table 3).
739 We also collapsed the behavioral data across animals to generate an average psychometric curve, and
740 computed its threshold. Despite the fact that neurometric and psychometric thresholds were derived in
741 different groups of animals, the two data sets were in close agreement (Figure 7f). The psychophysical
742 threshold of each individual ferret fell within the interquartile range of the neurometric distribution
743 (26.47th, 50.00th, and 67.65th percentiles of the distribution, respectively), and the estimated threshold
744 of the aggregate ferret behavior data was very close to the median of the neural distribution (47th
745 percentile, average psychometric function threshold: 32.22% coherence, median neural threshold:
746 34.63%). Thus, neural limits on motion integration imposed by PSS are in close agreement with the
747 behavioral observed limits. More work is necessary to fully establish the role of PSS and other visual
748 areas in complex motion processing, and to identify the areas involved in processing of Glass patterns in
749 ferrets. However, our findings represent a promising sign that at least the RDK task taps into functions
750 supported by the ferret's higher-level visual areas.

751

752

753 **Discussion**

754 To date, there have been few detailed behavioral studies on the visual capabilities of ferrets. Here, we
755 systematically tested their ability to discriminate simple gratings and more complex stimuli requiring
756 integration. The first important conclusion derived from our experiments is that ferrets are good
757 subjects for visual psychophysics. For all stimulus types tested, their performance systematically
758 depended on critical stimulus parameters such as spatial frequency or coherence level, in a way that
759 was well captured by standard psychometric functions. In addition, performance was reliable across
760 days, and ferrets usually performed a reasonable number of trials per day. Ferrets consistently were
761 able to perform tasks with low lapse rates. This is important, as it confirms that behavior is tightly
762 controlled by the stimulus. It is worth noting that to reliably achieve these low lapse rates, attention
763 needed to be paid to any response bias exhibited during training and testing. Individual animals at times
764 developed a preference for one of the two response ports, and chose it regardless of the stimulus.
765 Requiring the animals to end each trial by choosing the correct spout helped to significantly reduce the
766 occurrence of response biases. For the head-fixed behavior, it was additionally important to ensure that
767 all spouts were equally reachable by the animal. Any remaining biases could then be eliminated by
768 temporarily changing the reward ratio of the response spouts.

769 So far, head-fixed paradigms have not been used to investigate visual behavior in ferrets. Here, we
770 demonstrate that head-fixed and freely-moving behavior can be used equally well for vision research in
771 this species. The two paradigms have different advantages and disadvantages: While the freely-moving
772 paradigm lacks complete control over certain stimulus parameters (including viewing distance), it
773 mimics natural behavior, requires no cranial implants, and animals usually take to it quickly. It thus lends
774 itself to studies requiring screening of larger cohorts of animals. The head-fixed paradigm, on the other
775 hand, requires implants and takes longer to train, but provides complete control over viewing
776 conditions. Because of the fixed head position, it also lends itself more easily to combined recording and

777 behavior experiments, in particular if neural activity is to be recorded optically (e.g. using two-photon
778 calcium imaging).

779 In the experiments described here, we controlled the animal's head position and distance relative to
780 the screen, but did not attempt to monitor eye position. Using the head-fixed setup to record neural
781 activity in visual cortex while animals perform a task will require that the stimulus can be maintained at
782 a stable position relative to center of gaze, to ensure that stimuli remain within the receptive fields of
783 the neurons under study. Tracking of eye position is feasible in ferrets and could be added to the setup
784 (Stitt et al., 2018). This – at the minimum – would allow monitoring of eye position during an
785 experiment, which could be used to eliminate trials contaminated by saccades or large deviations in eye
786 position from a desired location. Monitoring of eye position might also enable tasks in which ferrets are
787 trained to fixate a target, which would more tightly control stimulus position. Fixation tasks likely will
788 also be required to be able to present stimuli peripherally. Whether ferrets can indeed be trained to
789 fixate a stimulus remains an open question to be investigated in future experiments. In any case, the
790 addition of eye tracking to the setup will require the development of efficient strategies to calibrate the
791 eye tracking signal, either by developing tasks that require ferrets to fixate targets presented at different
792 positions, or through other automated procedures like the ones developed for eye tracking in rats
793 (Zoccolan et al., 2010).

794 The second important conclusion derived from our experiments is that ferrets show clear behavioral
795 evidence of higher-level visual processing, as indicated by their ability to perform motion and form tasks
796 that require integration of information across multiple elements. The motion integration thresholds
797 measured here are consistent with the results of a previous ferret study, in which animals were tested
798 on their ability to discriminate coherent from random motion (Hupfeld et al., 2006). In this task, ferrets
799 achieved a performance level of 75% correct for coherence levels of around 20%. These thresholds are
800 lower than the thresholds of 30 - 37% determined here, most likely because of the simpler

801 discrimination task. The studies also differ in other parameters such as the lapse rates and the number
802 of trials performed per day, which might have affected the measured psychometric functions. Motion
803 integration thresholds have also been measured in the cat, a carnivore like the ferret, using stimuli very
804 similar to the ones employed here. Across two studies, motion integration thresholds for cats (measured
805 either at 70 or 75% correct performance) ranged from 5 to 15% (Mitchell et al., 2009; Rudolph and
806 Pasternak, 1996). These thresholds are lower than the ones measured for ferrets in this study, which
807 could indicate that cats are better able to integrate motion signals, but might also be due to differences
808 in the amount of training animals received in the different studies.

809 Ferrets were similarly able to perform a form integration task. Note that we chose to use linear
810 rather than concentric Glass patterns here to more closely match motion and form tasks. In human
811 subjects, thresholds for linear Glass patterns differ from those for more complex patterns containing
812 curvature, such as concentric Glass patterns (Wilson and Wilkinson, 1998; Wilson et al., 1997). It has
813 been proposed that this difference arises because Glass patterns containing curvature tap into the
814 curvature tuning in higher-level areas like V4 (Gallant et al., 1993; Pasupathy and Connor, 1999, 2001).
815 Yet, these conclusions might be confounded by effects of viewing Glass patterns through circular
816 apertures, as is commonly the case (Dakin and Bex, 2002). Nonetheless, probing form integration in
817 ferrets with curved Glass patterns remains an interesting topic for future investigations.

818 Generally, processing of RDK and Glass patterns has been associated with higher-level visual areas.
819 In monkeys, MT in particular has been considered central for the processing of RDK (Britten et al., 1992;
820 Newsome and Pare, 1988; Salzman et al., 1990). One important reason for this conclusion is the close
821 agreement between neurometric functions of MT neurons and behaviorally measured psychometric
822 functions (Britten et al., 1992; Shadlen et al., 1996). In contrast to the primate studies, we so far have
823 not recorded neurons and behavior simultaneously in ferrets doing motion or form integration tasks.
824 Yet, we have recently shown that PSS is a higher-level motion area exhibiting similar degrees of motion

825 integration as MT (Lempel and Nielsen, 2019). These findings, combined with the close agreement of
826 psychometric and PSS neurometric thresholds observed here, support the notion that performance on
827 the RDK task indeed depends on higher-level visual areas in ferrets as in primates. This would also be
828 consistent with the observation that PSS lesions impact ferrets on a motion detection task using RDK
829 (Hupfeld et al., 2007). Comparisons to the cat further support this argument, as lesions of cat
830 suprasylvian sulcus – a region containing motion areas that are likely closely related to ferret PSS
831 (Philipp et al., 2006)– similarly disrupt motion integration thresholds (Rudolph and Pasternak, 1996).
832 Ferrets ability to perform the form integration task then raises the intriguing possibility that there is a
833 matching higher-level visual area for form processing, to be located in future experiments.

834 Finally, it should be noted that testing ferrets on RDK and Glass patterns required certain
835 adjustments – in particular an increase of the dot sizes – relative to experiments in humans and non-
836 human primates to accommodate their poorer visual acuity. Our own experiments estimated peak
837 contrast sensitivity to fall around 0.18 cpd, and a maximum acuity of 0.65 cpd. As discussed above, these
838 behavioral acuity estimates are consistent with spatial frequency tuning curves of area 17 neurons in
839 ferrets (Baker et al., 1998). They also agree with an earlier behavioral study testing the ability of ferrets
840 to detect gratings of different spatial frequencies and contrasts (von Melchner et al., 2000).

841 In conclusion, our experiments firmly establish the feasibility of visual psychophysics in ferrets,
842 including on experiments thought to tap into higher-level visual functions. RDK and Glass patterns have
843 been used previously to study the development of motion and form vision pathways in monkeys and
844 humans (Grinter et al., 2010; Kiorpes et al., 2012; Maurer and Lewis, 2018). Our findings open the door
845 to perform similar experiments in ferrets. Because of their early birth (Sharma and Sur, 2014), and the
846 ability to systematically alter visual experience during development (e.g., Chapman and Gödecke, 2000;
847 Chapman and Stryker, 1993; Li et al., 2006; Van Hooser et al., 2012; White et al., 2001), this presents
848 exciting opportunities for future developmental research.

849 **References**

- 850 Baker, G., Thompson, I., Krug, K., Smyth, D., and Tolhurst, D. (1998). Spatial-frequency tuning and
851 geniculocortical projections in the visual cortex (areas 17 and 18) of the pigmented ferret. *Eur. J.*
852 *Neurosci.* *10*, 2657–68.
- 853 Born, R.T., and Bradley, D. (2005). Structure and Function of Visual Area MT. *Annu. Rev. Neurosci.* *28*,
854 157–189.
- 855 Brainard, D.H. (1997). The Psychophysics Toolbox. *Spat. Vis.* *10*, 433–436.
- 856 Britten, K.H., Shadlen, M.N., Newsome, W.T., and Movshon, J.A. (1992). The analysis of visual motion: a
857 comparison of neuronal and psychophysical performance. *J. Neurosci.* *12*, 4745–4765.
- 858 Busse, L., Ayaz, A., Dhruv, N.T., Katzner, S., Saleem, A.B., Schölvinck, M.L., Zaharia, A.D., and Carandini,
859 M. (2011). The Detection of Visual Contrast in the Behaving Mouse. *J. Neurosci.* *31*, 11351–11361.
- 860 Chapman, B., and Gödecke, I. (2000). Cortical Cell Orientation Selectivity Fails to Develop in the Absence
861 of ON-Center Retinal Ganglion Cell Activity. *J. Neurosci.* *20*, 1922–1930.
- 862 Chapman, B., and Stryker, M.P. (1993). Development of orientation selectivity in ferret visual cortex and
863 effects of deprivation. *J. Neurosci.* *13*, 5251.
- 864 Clopper, C.J., and Pearson, E.S. (1934). The Use of Confidence or Fiducial Limits Illustrated in the Case of
865 the Binomial. *Biometrika* *26*, 404–413.
- 866 Dakin, S.C., and Bex, P.J. (2002). Summation of concentric orientation structure: seeing the Glass or the
867 window? *Vision Res.* *42*, 2013–2020.
- 868 Dobbins, H.D., Marvit, P., Ji, Y., and Depireux, D.A. (2007). Chronically recording with a multi-electrode
869 array device in the auditory cortex of an awake ferret. *J. Neurosci. Methods* *161*, 101–111.
- 870 Doty, B.A., Jones, C.N., and Doty, L.A. (1967). Learning-Set Formation by Mink, Ferrets, Skunks, and Cats.
871 *Science* *155*, 1579–1580.
- 872 Eastman, K.M. (2012). PLDAPS: A Hardware Architecture and Software Toolbox for Neurophysiology
873 Requiring Complex Visual Stimuli and Online Behavioral Control. *Front. Neuroinformatics* *6*.
- 874 Efron, B., and Tibshirani, R. (1986). Bootstrap Methods for Standard Errors, Confidence Intervals, and
875 Other Measures of Statistical Accuracy. *Stat. Sci.* *1*, 54–75.
- 876 Fritz, J., Shamma, S., Elhilali, M., and Klein, D. (2003). Rapid task-related plasticity of spectrotemporal
877 receptive fields in primary auditory cortex. *Nat. Neurosci.* *6*, 1216.
- 878 Gallant, J.L., Braun, J., and Van Essen, D.C. (1993). Selectivity for polar, hyperbolic, and Cartesian gratings
879 in macaque visual cortex. *Science* *259*, 100–3.
- 880 Glass, L. (1969). Moiré effect from random dots. *Nature* *223*, 578–580.
- 881 Glass, L., and Pérez, R. (1973). Perception of Random Dot Interference Patterns. *Nature* *246*, 360–362.

- 882 Green, D.M., and Swets, J.A. (1966). Signal detection theory and psychophysics. (Oxford, England: John
883 Wiley).
- 884 Grinter, E.J., Maybery, M.T., and Badcock, D.R. (2010). Vision in developmental disorders: is there a
885 dorsal stream deficit? *Brain Res. Bull.* *82*, 147–60.
- 886 Hoel, P., Port, S., and Stone, C. (1971). Introduction to Statistical Theory. (Boston: Houghton, Mifflin), p.
887 83ff.
- 888 Hollensteiner, K.J. (2015). Crossmodal Integration Improves Sensory Detection Thresholds in the Ferret.
889 *PLoS One* *10*, e0124952.
- 890 Homman-Ludiye, J., Manger, P., and Bourne, J.A. (2010). Immunohistochemical parcellation of the ferret
891 (*Mustela putorius*) visual cortex reveals substantial homology with the cat (*Felis catus*). *J. Comp. Neurol.*
892 *518*, 4439–62.
- 893 Hupfeld, D., Distler, C., and Hoffmann, K.-P. (2006). Motion perception deficits in albino ferrets (*Mustela*
894 *putorius furo*). *Vision Res.* *46*, 2941–2948.
- 895 Hupfeld, D., Distler, C., and Hoffmann, K.-P. (2007). Deficits of visual motion perception and optokinetic
896 nystagmus after posterior suprasylvian lesions in the ferret (*Mustela putorius furo*). *Exp. Brain Res.* *182*,
897 509–523.
- 898 Kiorpes, L. (2016). The Puzzle of Visual Development: Behavior and Neural Limits. *J. Neurosci.* *36*,
899 11384–11393.
- 900 Kiorpes, L., Price, T., Hall-Haro, C., and Anthony Movshon, J. (2012). Development of sensitivity to global
901 form and motion in macaque monkeys (*Macaca nemestrina*). *Vision Res.* *63*, 34–42.
- 902 Kiper, D.C., and Kiorpes, L. (1994). Suprathreshold contrast sensitivity in experimentally strabismic
903 monkeys. *Vision Res.* *34*, 1575–1583.
- 904 Kleiner, M., Brainard, D., Pelli, D., Ingling, A., Murray, R., and Broussard, C. (2007). What's new in
905 psychtoolbox-3. *Perception* *36*, 1–16.
- 906 Lempel, A.A., and Nielsen, K.J. (2019). Ferrets as a Model for Higher-Level Visual Motion Processing.
907 *Curr. Biol.* *29*, 1–13.
- 908 Lewis, T.L., Ellemberg, D., Maurer, D., Dirks, M., Wilkinson, F., and Wilson, H.R. (2004). A Window on the
909 Normal Development of Sensitivity to Global Form in Glass Patterns. *Perception* *33*, 409–418.
- 910 Li, Y., Fitzpatrick, D., and White, L.E. (2006). The development of direction selectivity in ferret visual
911 cortex requires early visual experience. *Nat. Neurosci.* *9*, 676–681.
- 912 Marbach, F., and Zador, A.M. (2017). A self-initiated two-alternative forced choice paradigm for head-
913 fixed mice. *BioRxiv* 073783.
- 914 Maurer, D., and Lewis, T.L. (2018). Visual Systems. In *The Neurobiology of Brain and Behavioral*
915 *Development*, R. Gibb, and B. Kolb, eds. (Academic Press), pp. 213–233.

- 916 von Melchner, L., Pallas, S.L., and Sur, M. (2000). Visual behaviour mediated by retinal projections
917 directed to the auditory pathway. *Nature* **404**, 871–876.
- 918 Mitchell, D.E., Kennie, J., and Kung, D. (2009). Development of global motion perception requires early
919 postnatal exposure to patterned light. *Curr. Biol. CB* **19**, 645–649.
- 920 Newsome, W.T., and Pare, E.B. (1988). A selective impairment of motion perception following lesions of
921 the middle temporal visual area (MT). *J. Neurosci.* **8**, 2201–2211.
- 922 Orban, G. (2008). Higher Order Visual Processing in Macaque Extrastriate Cortex. *Physiol. Rev.* **88**, 59 –
923 89.
- 924 Pasupathy, A., and Connor, C.E. (1999). Responses to contour features in macaque area V4. *J.*
925 *Neurophysiol.* **82**, 2490–502.
- 926 Pasupathy, A., and Connor, C.E. (2001). Shape representation in area V4: position-specific tuning for
927 boundary conformation. *J. Neurophysiol.* **86**, 2505–19.
- 928 Pelli, D.G. (1997). The VideoToolbox software for visual psychophysics: transforming numbers into
929 movies. *Spat. Vis.* **10**, 437–442.
- 930 Philipp, R., Distler, C., and Hoffmann, K.-P. (2006). A Motion-sensitive Area in Ferret Extrastriate Visual
931 Cortex: an Analysis in Pigmented and Albino Animals. *Cereb. Cortex* **16**, 779–790.
- 932 Pilly, P.K., and Seitz, A.R. (2009). What a difference a parameter makes: A psychophysical comparison of
933 random dot motion algorithms. *Vision Res.* **49**, 1599–1612.
- 934 Pollard, J.S., Beale, I.L., Lysons, A.M., and Preston, A.C. (1967). Visual Discrimination in the Ferret.
935 *Percept. Mot. Skills* **24**, 279–282.
- 936 Pontenagel, T., and Schmidt, U. (1980). Untersuchungen zur Leistungsfähigkeit des Gesichtssinnes beim
937 Frettchen, *Mustela putorius f. furo* L. *Z. F. Säugetierkunde* **45**, 376–383.
- 938 Prins, N., and Kingdom, F.A.A. (2018). Applying the Model-Comparison Approach to Test Specific
939 Research Hypotheses in Psychophysical Research Using the Palamedes Toolbox. *Front. Psychol.* **9**.
- 940 Rudolph, K.K., and Pasternak, T. (1996). Lesions in Cat Lateral Suprasylvian Cortex Affect the Perception
941 of Complex Motion. *Cereb. Cortex* **6**, 814–822.
- 942 Salzman, C., Britten, K., and Newsome, W. (1990). Cortical microstimulation influences perceptual
943 judgements of motion direction. *Nature* **346**, 174–177.
- 944 Schütz, A.C., Braun, D.I., Movshon, J.A., and Gegenfurtner, K.R. (2010). Does the noise matter? Effects of
945 different kinematogram types on smooth pursuit eye movements and perception. *J. Vis.* **10**, 26–26.
- 946 Shadlen, M.N., Britten, K.H., Newsome, W.T., and Movshon, J.A. (1996). A computational analysis of the
947 relationship between neuronal and behavioral responses to visual motion. *J. Neurosci.* **16**, 1486–1510.

- 948 Sharma, J., and Sur, M. (2014). The Ferret as a Model for Visual System Development and Plasticity. In
949 *Biology and Diseases of the Ferret*, (John Wiley & Sons, Ltd), pp. 711–734.
- 950 Stitt, I., Zhou, Z.C., Radtke-Schuller, S., and Fröhlich, F. (2018). Arousal dependent modulation of
951 thalamo-cortical functional interaction. *Nat. Commun.* 9, 2455.
- 952 Ungerleider, L.G., and Pasternak, T. (2004). Ventral and dorsal cortical processing streams. In *The Visual*
953 *Neurosciences*, (Cambridge: MIT Press), pp. 541–562.
- 954 Van Hooser, S.D., Li, Y., Christensson, M., Smith, G.B., White, L.E., and Fitzpatrick, D. (2012). Initial
955 neighborhood biases and the quality of motion stimulation jointly influence the rapid emergence of
956 direction preference in visual cortex. *J. Neurosci.* 32, 7258–66.
- 957 White, L.E., Coppola, D.M., and Fitzpatrick, D. (2001). The contribution of sensory experience to the
958 maturation of orientation selectivity in ferret visual cortex. *Nature* 411, 1049–1052.
- 959 Wichmann, F.A., and Hill, N.J. (2001). The psychometric function: I. Fitting, sampling, and goodness of fit.
960 *Percept. Psychophys.* 63, 1293–1313.
- 961 Wilson, H.R., and Wilkinson, F. (1998). Detection of global structure in Glass patterns: implications for
962 form vision. *Vision Res.* 38, 2933–2947.
- 963 Wilson, H.R., Wilkinson, F., and Asaad, W. (1997). Concentric orientation summation in human form
964 vision. *Vision Res.* 37, 2325–2330.
- 965 Zoccolan, D., Graham, B.J., and Cox, D.D. (2010). A Self-Calibrating, Camera-Based Eye Tracker for the
966 Recording of Rodent Eye Movements. *Front. Neurosci.* 4.
- 967
- 968

969 **Figure legends**

970 **Figure 1: Freely-moving setup and basic stimulus design**

971 **(a)** Schematic of freely-moving behavioral setup. The trial initiation port was centered on the wall
972 opposite the visual display. Choice ports were on either side of the display. An IR beam was also placed
973 across the middle of the box.

974 **(b)** Task structure. An LED was illuminated above the trial initiation port to signal that the ferret could
975 initiate a trial. When the ferret broke the IR beam in that port, a small reward was dispensed, and
976 stimulus presentation was triggered. Subsequent selection of the correct port resulted in ending
977 stimulus presentation and reward delivery.

978 **(c)** Acuity task stimuli: Sinusoidal gratings with varying contrasts and spatial frequencies. The ferrets
979 were trained to discriminate horizontal from vertical gratings.

980 **(d)** Motion integration task stimuli: RDK consisting of black and white dots with varying coherence
981 levels. RDK had to be discriminated based on their direction of motion (left or right).

982 **(e)** Form integration task stimuli: Linear Glass patterns with varying degrees of coherence. The ferrets
983 were trained to discriminate horizontal from vertical patterns.

984

985 **Figure 2: Behavioral estimates of visual acuity**

986 **(a)** Psychometric curves for one ferret (F4) for three spatial frequencies. Error bars represent 95%
987 confidence intervals (see Methods).

988 **(b)** Psychometric curves fit to data from individual testing sessions using a spatial frequency of 0.18 cpd
989 (ferret F4). 13 sessions are shown here.

990 **(c)** Contrast sensitivity curves for each ferret. Error bars represent 68% confidence intervals (see
991 Methods).

992

993 **Figure 3: Motion integration thresholds**

994 **(a)** Psychometric curves for each ferret on the motion integration task (dot speed 48 deg/s). Error bars
995 represent 95% confidence intervals.

996 **(b)** Impact of training on motion integration thresholds: Performance for F4 at the time of initial
997 threshold measurements, and after 11 additional sessions.

998 **(c)** Sided coherence threshold Δ as a function of dot speed for each ferret.

999 **(d)** Performance of ferret F4 for RDK of 60% coherence as a function of dot speed.

1000 **(e)** Performance comparison for short versus infinite dot lifetime (data for ferret F0).

1001 **(f)** Performance comparison for white dots on a black background versus black and white dots on a gray
1002 background (data for ferret F6).

1003

1004 **Figure 4: Head-fixed behavior paradigm.**

1005 **(a)** Schematic drawing of the head-fixed behavior setup (top view). The setup consisted of 3 major
1006 components, a body holder, head-post holder, and the reward spouts. All three components could be
1007 moved relative to each other to allow the animal to assume a comfortable posture while in the setup,
1008 and to reach the spouts easily. Each spout could be moved independently between a retracted and a
1009 forward position by means of a gas piston. Animals could only lick the spouts when in the forward
1010 position. All spouts were mounted on a large translation stage to control their overall distance from the
1011 animal. In addition, the two peripheral spouts were mounted on two smaller translation stages to
1012 control the lateral distance between the spouts. This was necessary to make sure that animals could not
1013 activate more than one spout simultaneously.

1014 **(b)** Side-view of the head-fixed behavior setup.

1015 **(c)** Three-spout task design. A trial initiation cue was presented and the center spout was moved
1016 forward. When the ferret licked the center spout, a small reward was dispensed. Next, the center spout

1017 was retracted and stimulus presentation was triggered. The two choice spouts were moved forward. If
1018 the ferret licked the correct spout first, the incorrect spout was retracted, the stimulus removed, and
1019 the ferret received a large water reward. If the ferret contacted the incorrect spout first, it was also
1020 retracted. The ferret then had to contact the correct spout (which remained in position) to end the trial
1021 and receive a much smaller reward.

1022

1023 **Figure 5: Comparison of motion integration thresholds measured using head-fixed and freely-moving**
1024 **paradigms.**

1025 Psychometric curves from all ferrets for the motion integration task at 72 deg/s. Colored lines show the
1026 performance of the head-fixed animals, F8 and F9. Black lines show the performance of freely moving
1027 animals (F0, F4 and F6). Error bars represent 95% confidence intervals.

1028

1029 **Figure 6: Form integration thresholds measured using Glass patterns.**

1030 Psychometric curves for Glass pattern stimuli for two ferrets. Error bars represent 95% confidence
1031 intervals.

1032

1033 **Figure 7: Comparison of neurometric and psychometric motion integration thresholds.**

1034 **(a)** Sagittal view of the ferret brain, with the suprasylvian sulcus (SS) and PSS indicated.

1035 **(b)** Firing rate distributions for an example PSS neuron, evoked by RDK of different coherence levels
1036 moving in the neurons preferred direction (black bars) or its null direction (white bars). Each bar
1037 indicates the number of trials on which a neuron exhibited a particular firing rate.

1038 **(c)** ROC curves generated from the distributions in (b).

1039 **(d)** aROC values for all directionally selective and significantly responsive neurons (N = 36) at 100%
1040 coherence. Red dashed line at 0.75 indicates criterion cut-off.

1041 **(e)** Comparison of an example neurometric function, computed for the neuron shown in (c) and (d), to
1042 the average psychometric function. The average psychometric function was generated by fitting
1043 behavioral data collapsed across all 3 ferrets tested in the freely-moving paradigm. The threshold for the
1044 average psychometric function, using a criterion of 75% correct responses, is also indicated.

1045 **(f)** Distribution of 75% correct coherence thresholds across all directionally selective, significantly
1046 responsive neurons with aROC values of 0.75 or above at 100% coherence (N = 34). Also shown are the
1047 mean of this distribution, the threshold based on the average psychometric function (see (e)), and the
1048 thresholds of each of the three ferrets, all using the same criterion of 75% correct.

1049

1050 **Table 1** Tasks that each ferret performed. All ferrets learned the acuity task followed by the RDK task
1051 and then the Glass pattern task.

1052

1053 **Table 2:** Peak contrast sensitivity and maximum acuity estimates. Mean reported with standard error.

1054

1055 **Table 3:** Threshold evaluations for each complex visual task. Hf – head-fixed behavior. Free – freely-
1056 moving behavior. Mean reported with standard error.

1057

Ferret	Acuity	Dots	Glass
F0	X	X	X
F4	X	X	
F2	X		
F6		X	X
F8		X	
F9		X	

1058

1059 Table 1

1060

Ferret	Peak Contrast Sensitivity (cpd)	Maximum Acuity Estimate (cpd)	No. Trials	No. Sessions
F0	0.17	0.70	1420	11
F2	0.17	0.60	1500	17
F4	0.20	0.65	1291	13
Mean	0.18 +/- 0.01	0.65 +/- 0.03	1404 +/- 61	14 +/- 2

Table 2

1064

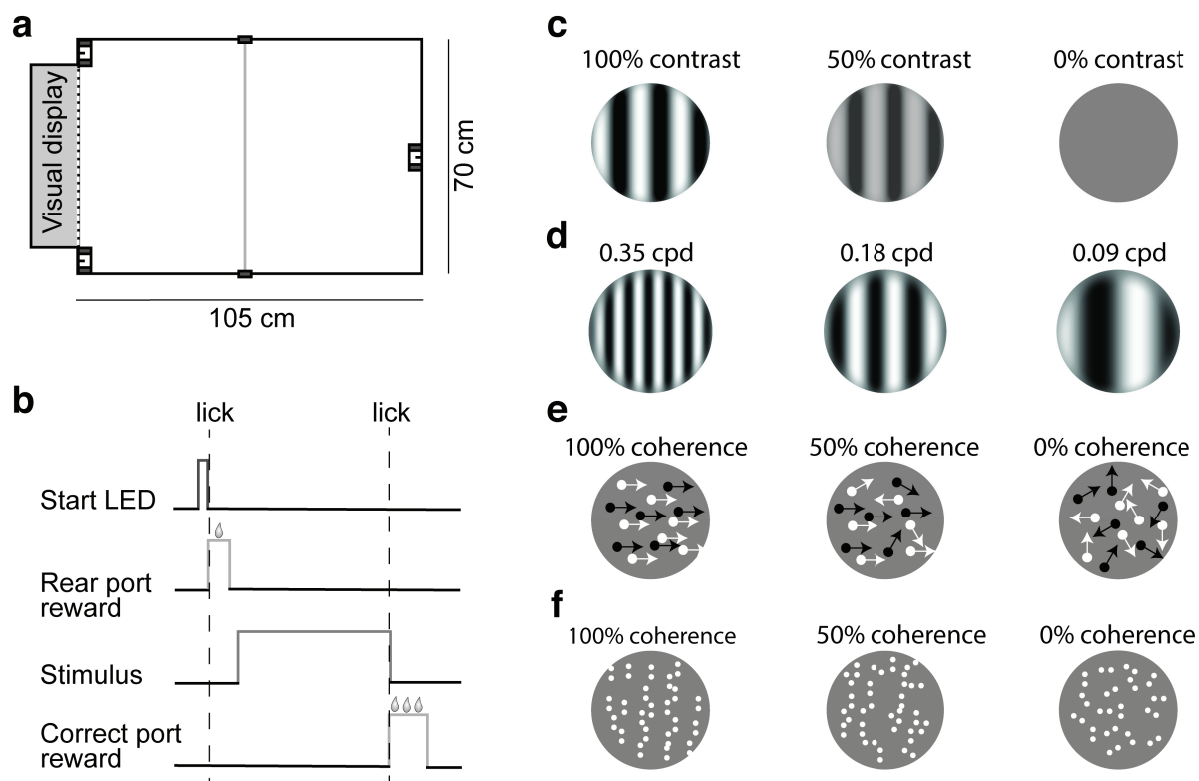
Task	Δ (50 – 68%)	Threshold at 75%	Threshold at 82%	No. Trials	No. Sessions
Dots, 72°/s					
F0	20.06%	35.62%	45.07%	1371	12
F4	14.05%	23.39%	32.17%	503	6
F6	12.79%	26.74%	34.98%	778	7
Mean, free	15.63 +/- 2.24%	28.58 +/- 2.65%	37.40 +/- 3.92%	884 +/- 256	8 +/- 2
F9 (hf)	18.36%	30.55%	41.62%	568	4
F8 (hf)	28.35%	45.27%	59.48%	939	2
Mean, hf	23.36 +/- 5.00%	37.91 +/- 7.36%	50.55 +/- 8.93%	753 +/- 186	3 +/- 1
Mean, all	18.72 +/- 2.75%	32.31 +/- 3.83%	42.66 +/- 4.79%	832 +/- 155	6 +/- 2
Dots, 48°/s					
F0	18.93%	42.96%	49.98%	308	3
F4	15.01%	25.10%	35.56%	581	5
F6	18.91%	34.51%	47.76%	707	8
Mean	17.62 +/- 1.30%	34.19 +/- 5.16%	44.43 +/- 4.48%	532 +/- 118	5 +/- 1
Dots, 24°/s					
F0	19.89%	38.37%	50.89%	570	5
F4	17.67%	39.16%	47.37%	492	5
F6	16.67%	33.97%	44.20%	749	8
Mean	18.07 +/- 0.95%	37.16 +/- 1.61%	47.49 +/- 1.93%	604 +/- 76	6 +/- 1
Glass					
F0	21.32%	44.31%	66.68%	766	6
F6	23.25%	48.94%	65.45%	616	5
Mean	22.28 +/- 0.97%	46.65 +/- 2.34%	66.06 +/- 0.62%	691 +/- 75	6 +/- 1

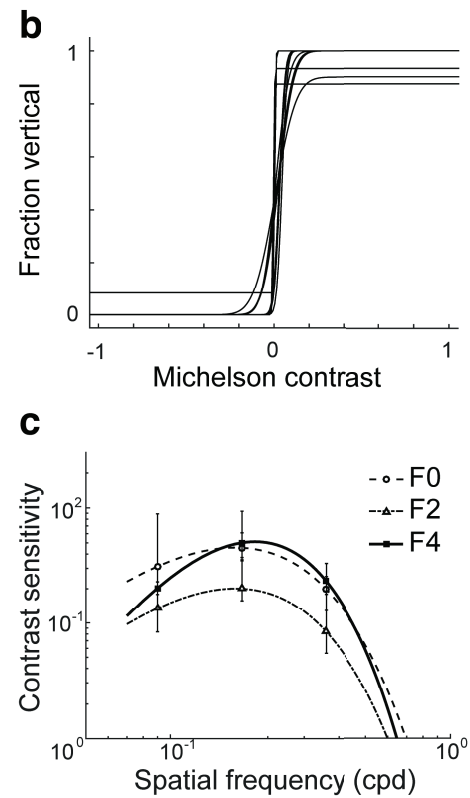
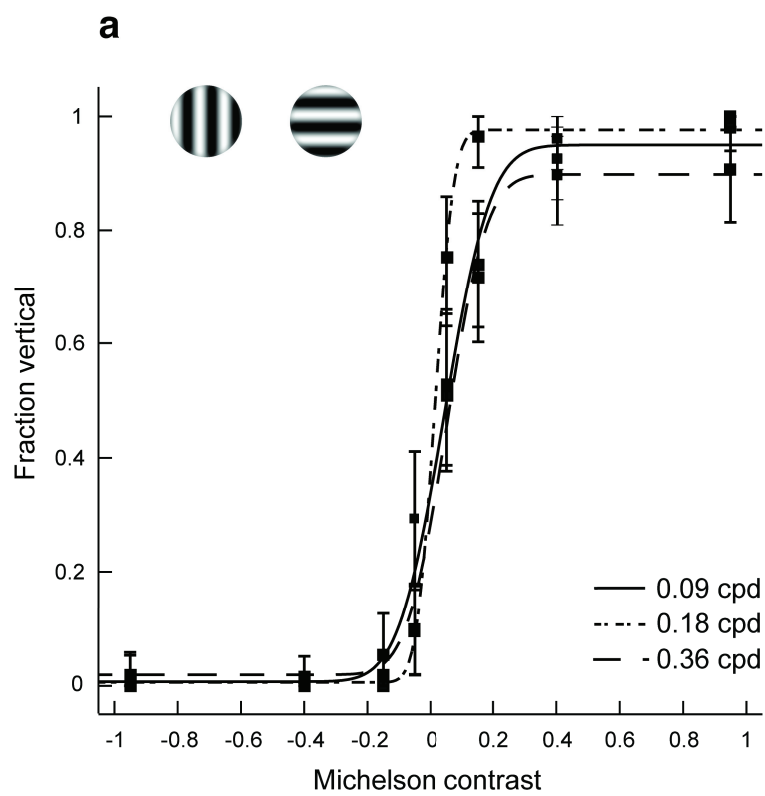
1065

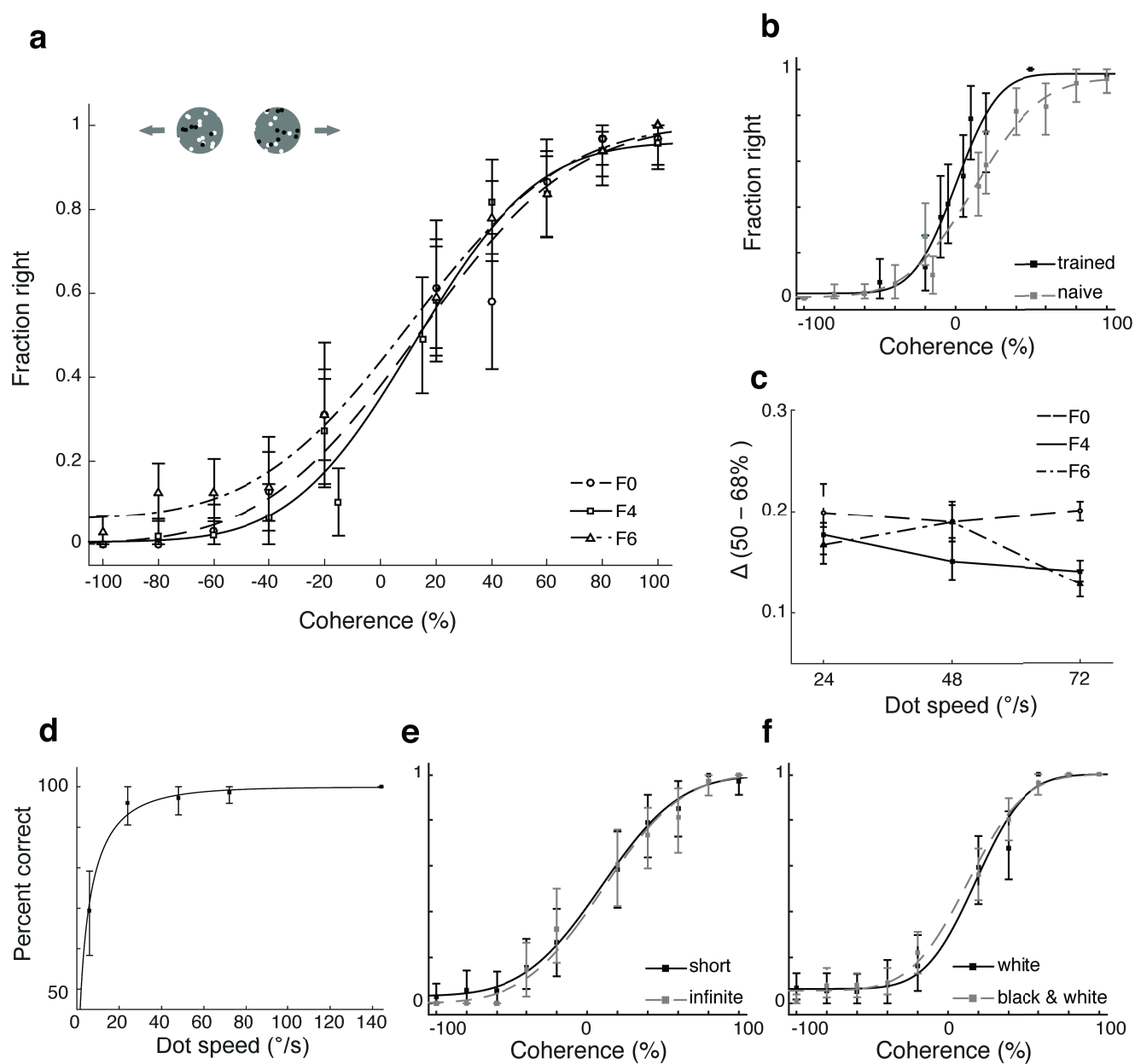
1066

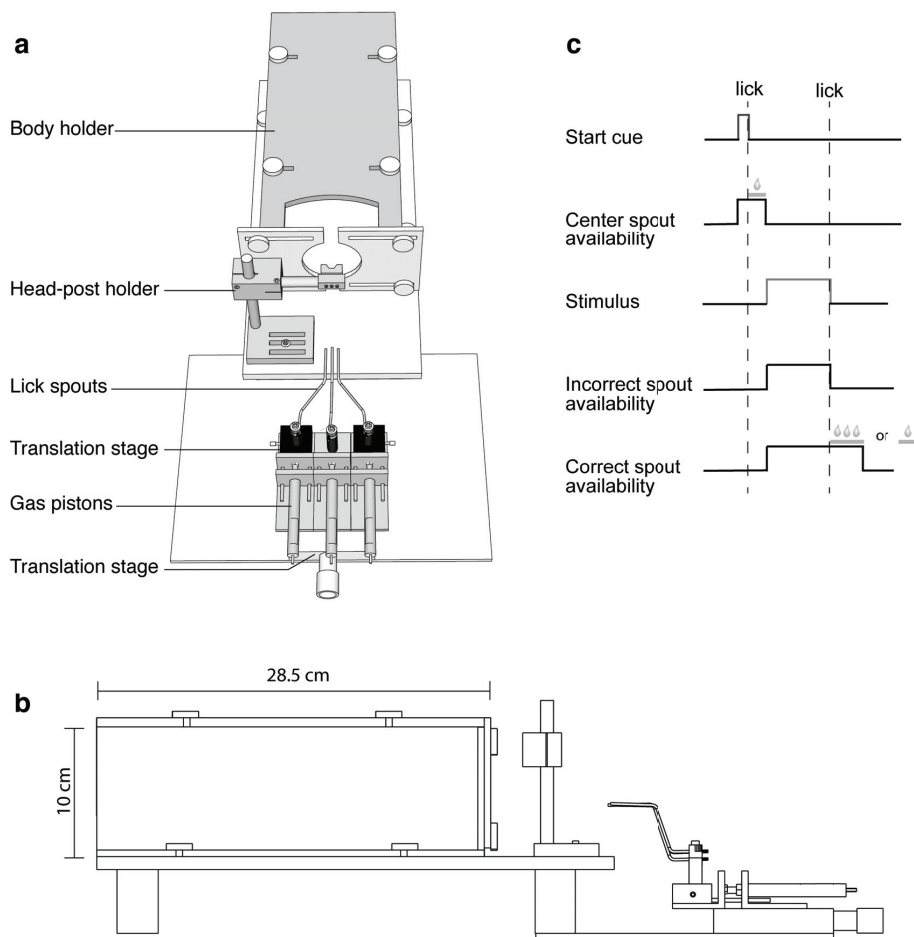
1067 Table 3

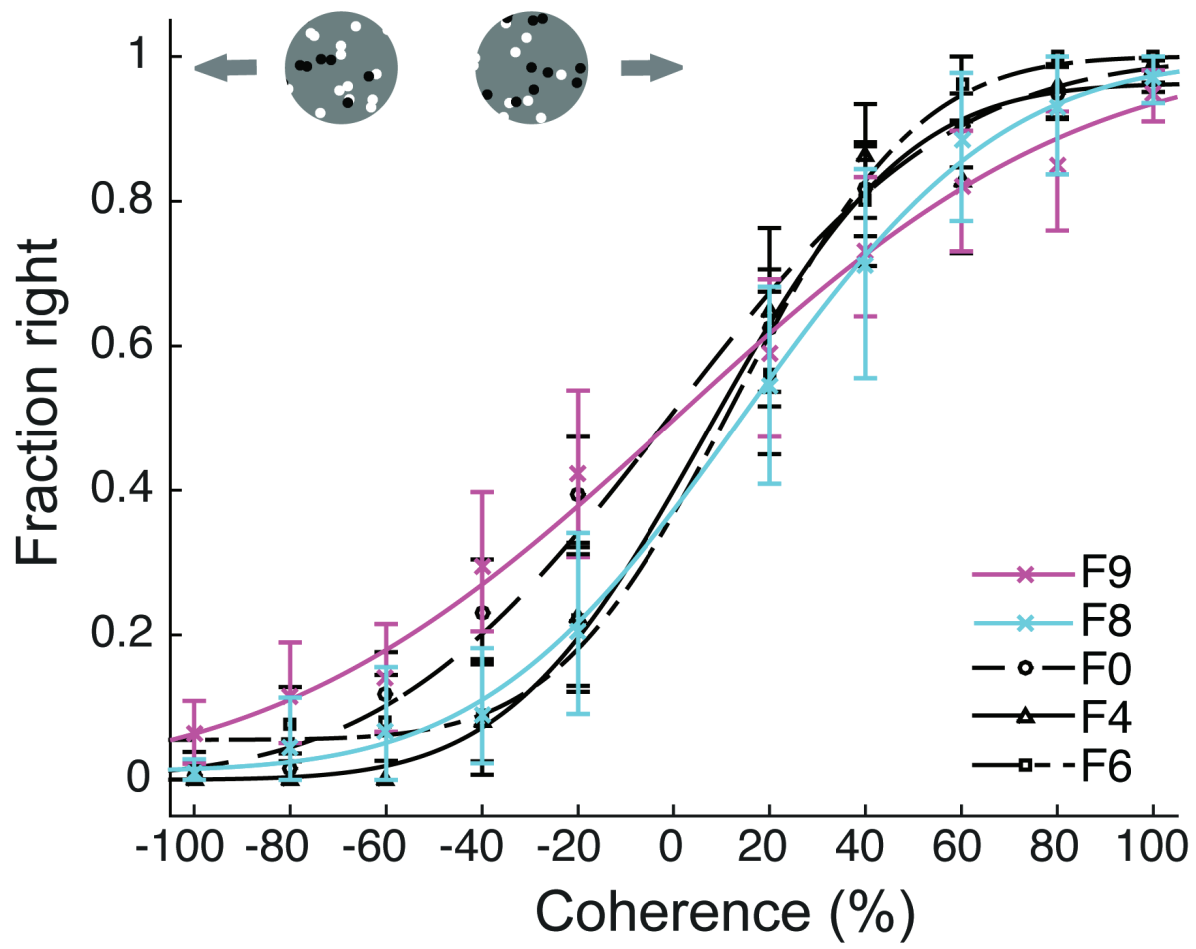
1068

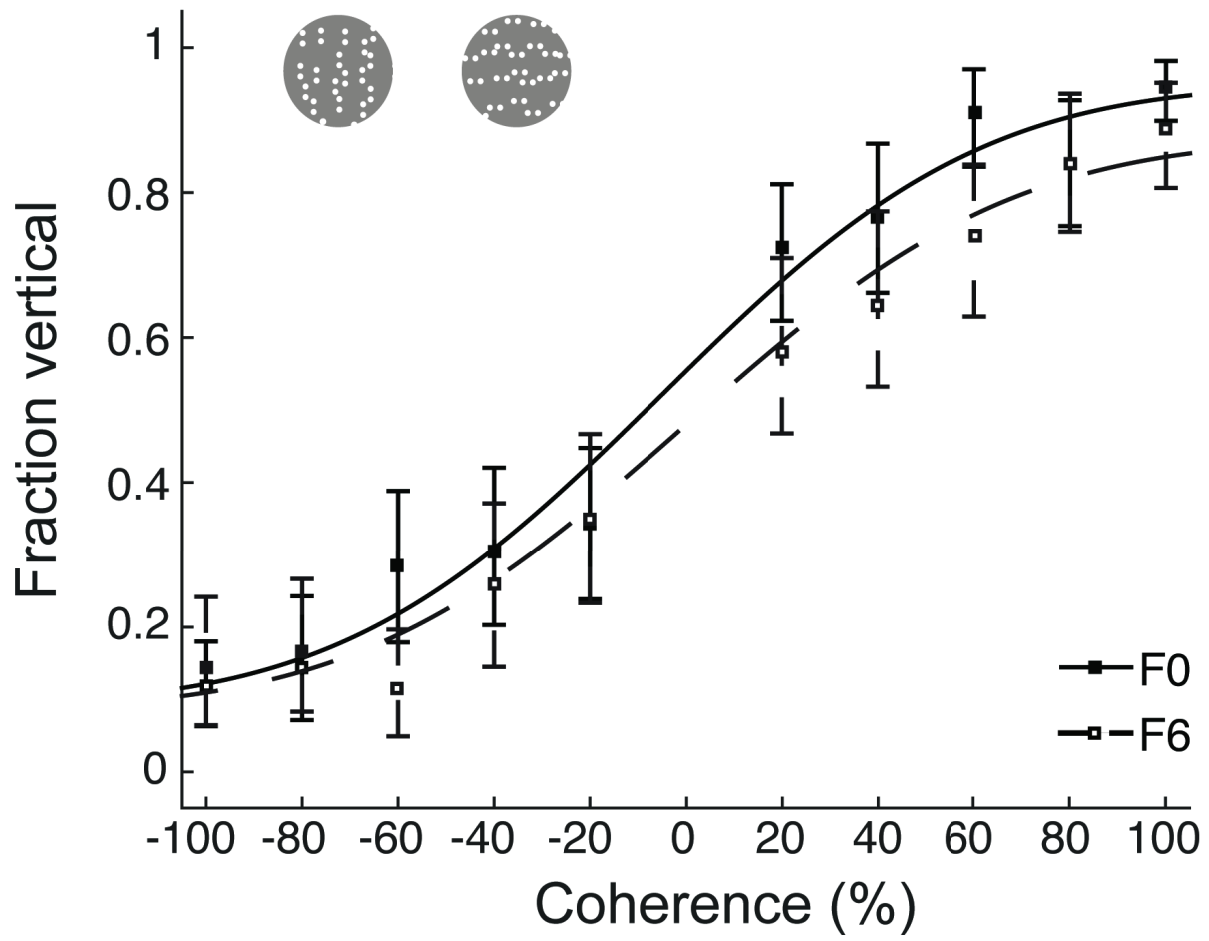




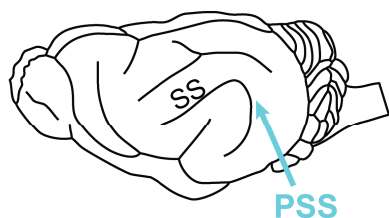




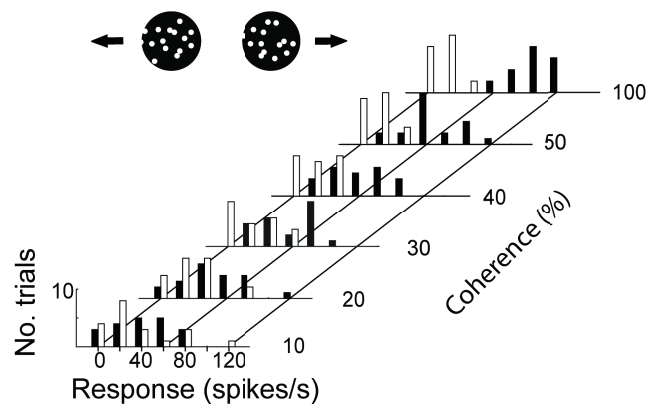




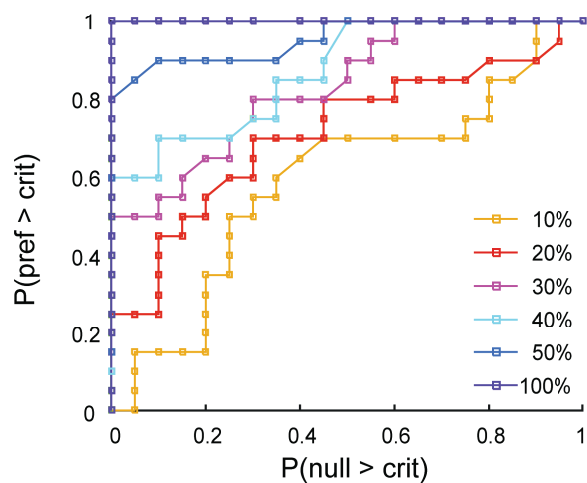
a



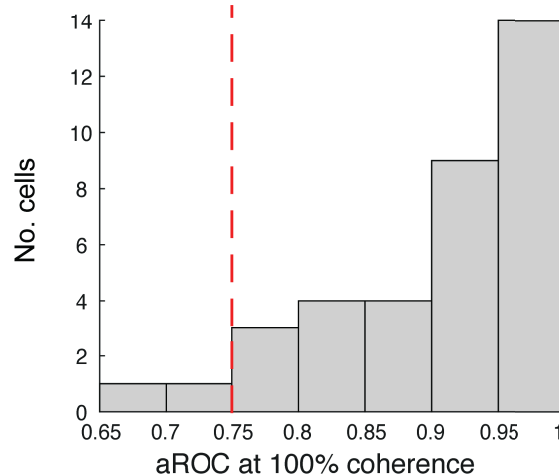
b



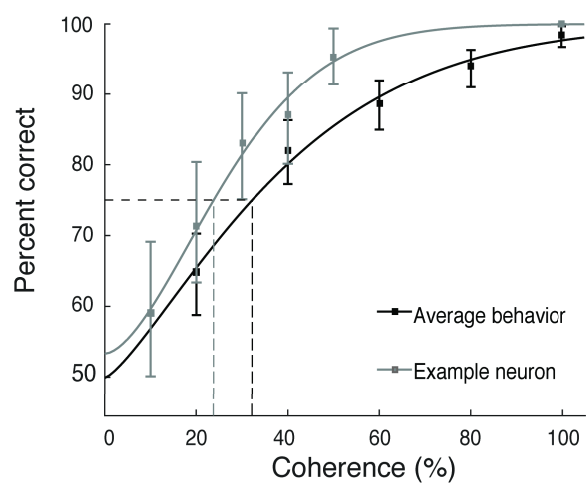
c



d



e



f

